

1
2
3
4
5
6 **The Ca²⁺-calmodulin-Ca²⁺/calmodulin-dependent protein kinase II**
7 **pathway is involved in oxidative stress-induced mitochondrial**
8 **permeability transition and apoptosis in isolated rat hepatocytes**
9
10
11
12
13
14
15
16
17

18 FLAVIA D. TOLEDO¹, LEONARDO M. PÉREZ¹, CECILIA L. BASIGLIO¹,

19
20 ENRIQUE J. SANCHEZ POZZI¹ AND MARCELO G. ROMA¹
21
22
23
24
25
26
27
28
29
30
31

32
33 ¹*Instituto de Fisiología Experimental, CONICET-Universidad de Rosario, ARGENTINA.*
34
35
36
37
38
39
40
41
42
43
44

45 **Author for correspondence:**

46 Dr. Marcelo G. Roma

47 Instituto de Fisiología Experimental (IFISE)

48 Facultad de Ciencias Bioquímicas y Farmacéuticas

49 Suipacha 570, 2000 – Rosario, ARGENTINA

50 Tel.: +54-341-4305799

51 Fax: +54-341-4399473

52 E-mail: mroma@fbioyf.unr.edu.ar
53
54
55
56
57
58
59
60
61
62
63
64
65

1
2
3
4
5
6
7
8
9
10
11
12
13
14
15
16
17
18
19
20
21
22
23
24
25
26
27
28
29
30
31
32
33
34
35
36
37
38
39
40
41
42
43
44
45
46
47
48
49
50
51
52
53
54
55
56
57
58
59
60
61
62
63
64
65

ABSTRACT

Oxidative stress is a common event in most hepatopathies, leading to mitochondrial permeability transition pore (MPTP) formation and further exacerbation of both oxidative stress from mitochondrial origin and cell death. Intracellular Ca^{2+} elevations play a permissive role in these events, but the underlying mechanisms are poorly known. We examined in primary cultured rat hepatocytes whether the Ca^{2+} /calmodulin (CaM)-dependent protein kinase II (CaMKII) signalling pathway is involved in this process, by using *tert*-butyl hydroperoxide (*t*BOOH) as a pro-oxidizing, model compound. *t*BOOH (500 μM , 15 min) induced MPTP formation, as assessed by measuring mitochondrial membrane depolarization as a surrogate marker, and increased lipid peroxidation in a cyclosporin A (CsA)-sensitive manner, revealing the involvement of MPTPs in *t*BOOH-induced ROS formation. Intracellular Ca^{2+} sequestration with BAPTA/AM, CaM blockage with W7 or trifluoperazine, and CaMKII inhibition with KN-62 all fully prevented *t*BOOH-induced MPTP opening and reduced *t*BOOH-induced lipid peroxidation to a similar extent to CsA, suggesting that Ca^{2+} /CaM/CaMKII signaling pathway fully mediates MPTP-mediated mitochondrial ROS generation. *t*BOOH induced apoptosis, as shown by flow cytometry of annexin V/propidium iodide, mitochondrial release of cytochrome *c*, activation of caspase-3 and increase in the Bax-to-Bcl-xL ratio, and the Ca^{2+} /CaM/CaMKII signaling antagonists fully prevented these effects. Intramitochondrial CaM and CaMKII were partially involved in *t*BOOH-induced MPTP formation, since W7 and KN-62 both attenuated the *t*BOOH-induced, MPTP-mediated swelling of isolated mitochondria. We concluded that Ca^{2+} /CaM/CaMKII

1
2
3
4
5
6
7
8
9
10
11
12
13
14
15
16
17
18
19
20
21
22
23
24
25
26
27
28
29
30
31
32
33
34
35
36
37
38
39
40
41
42
43
44
45
46
47
48
49
50
51
52
53
54
55
56
57
58
59
60
61
62
63
64
65

signaling pathway is a key mediator of oxidative stress-induced induced MPTP formation, and the subsequent exacerbation of oxidative stress from mitochondrial origin and apoptotic cell death.

1
2
3
4
5
6
7
8
9
10
11
12
13
14
15
16
17
18
19
20
21
22
23
24
25
26
27
28
29
30
31
32
33
34
35
36
37
38
39
40
41
42
43
44
45
46
47
48
49
50
51
52
53
54
55
56
57
58
59
60
61
62
63
64
65

Keywords:

Oxidative stress

tert-butyl hydroperoxide

Ca²⁺/Calmodulin -dependent protein kinase II

Mitochondrial permeability transition pore

Apoptosis

Cytochrome *c*

INTRODUCTION

Radical oxygen species (ROS) occurring under oxidative stress (OS) conditions plays a pivotal role in a wide variety of pathophysiological conditions (Muriel 2009), by oxidizing membrane phospholipids, proteins and nucleic acids (Cochrane 1991). The cellular alterations induced by this redox imbalance depend on the intensity and duration of the oxidative injury. High levels of OS lead predominantly to dramatic changes in plasma membrane permeability, release of cytosolic and mitochondrial components, impaired mitochondrial adenosine triphosphate (ATP) production and, finally, necrosis. Contrarily, lower levels of OS unable to deplete ATP levels cause apoptosis, since apoptosis is an energy-requiring process (Eguchi 1997).

Opening of mitochondrial permeability transition pores (MPTPs) under OS conditions has been implicated as a key, causative event in both manners of cell death. MPTP occurs by the dynamic association of a multiprotein complex of constitutive and regulatory proteins at the sites where the outer mitochondrial membrane is in contact with the inner mitochondrial membrane. The nature of this complex is uncertain, but it may involve a number of putative constitutive proteins such as the voltage dependent anion channel (VDAC) in the outer membrane, adenine nucleotide translocase (ANT), F_0/F_1 ATP synthase, and the phosphate carrier (PiC) in the inner membrane, and some regulatory proteins, such as cyclophilin D and complement component 1, q subcomponent binding protein (C1QBP), localized in the matrix; from all of them, only cyclophilin D has held up to genetic scrutiny as an essential protein involved in MPTP formation (Elrod 2013). MPTP opening leads to an abrupt increase in the permeability of the inner mitochondrial

1
2
3
4 membrane to small molecular weight solutes (< 1500 Da); this collapses ion gradients
5
6 across the inner mitochondrial membrane, leading to mitochondrial depolarization,
7
8 uncoupling of oxidative phosphorylation and, eventually, ATP depletion (Jeong 2008;
9
10 Imberti 1993). MPTP onset also causes mitochondrial swelling, with rupture of the
11
12 mitochondrial outer membrane and release of cytochrome *c* and other pro-apoptotic
13
14 molecules from the inter-membrane space to the cytosol (*e.g.*, apoptosis inducing factor,
15
16 Smac/Diablo). These molecules, together with other cytosolic factors, set off a cascade of
17
18 caspase activity that leads to apoptotic cell death (Jeong 2008). Alternatively, the release of
19
20 these proteins may occur through specific changes in the outer membrane permeability, by
21
22 translocation from cytosol of pro-apoptotic, pore-forming proteins such, as Bax and Bid
23
24 (Korsmeyer 2000).
25
26
27
28
29

30
31 Appart from governing cell death, MPTPs aggravates the initial OS that triggers its
32
33 primary onset. This occurs by (a) MPTP-induced loss of cytochrome *c*, which impairs the
34
35 flow of electrons in the respiratory chain inducing overreduction of the complexes and
36
37 leakage of electrons to the cytosol, (b) reduction of the electron acceptor, NAD⁺, which
38
39 results in ROS emission from the α -ketoglutarate dehydrogenase complex, and (c) loss of
40
41 glutathione from the matrix, which decreases the mitochondrial capacity to scavenge ROS
42
43 (Chinopoulos 2006).
44
45
46
47

48 Another major feature of the oxidative injury is the increase in cytosolic, free Ca²⁺
49
50 levels; this activates Ca²⁺-dependent degradative enzymes, such as phospholipases,
51
52 proteases and endonucleases, which play a major role in the onset of cell death (Orrenius
53
54 1992). In addition, cellular Ca²⁺ elevations exacerbates OS-induced cell death (Thor 1984),
55
56 by potentiating the capability of ROS to onset MPTP opening (Byrne 1999). Some
57
58
59
60
61
62
63
64
65

1
2
3
4 hypotheses have been advanced to explain this fact, although any of them have been proved
5
6 conclusively as yet. OS causes release of matrix Ca^{2+} that can be taken up back into the
7
8 mitochondria (Ca^{2+} cycling); this excessive Ca^{2+} cycling has been proposed to be
9
10 responsible for MPTP onset (Takeyama 1993). In addition, elevations of mitochondrial
11
12 matrix free Ca^{2+} may increase mitochondrial respiration, which is controlled by Ca^{2+} -
13
14 regulated mitochondrial dehydrogenases. This latter process may overstimulate
15
16 mitochondrial ROS production, thus triggering MPTP by oxidation of free thiol groups in
17
18 ANT, which increases the affinity of this protein for cyclophilin D to induce MPTP
19
20 generation (Kanno 2004). In addition, OS greatly enhances MPTP sensitivity to Ca^{2+} . This
21
22 occurs both by increasing cyclophilin D binding to ANT, a critical step in MPTP formation,
23
24 and by reducing the affinity of the intramitochondrial adenine nucleotide-binding site on
25
26 ANT; the binding of adenine nucleotides to this site inhibits competitively Ca^{2+} -dependent
27
28 MPTP formation (Halestrap 2000). Therefore, cellular Ca^{2+} overload occurring under OS
29
30 conditions would represent a vicious circle by which Ca^{2+} and ROS mutually potentiate
31
32 each other to exacerbate ROS formation from mitochondrial origin, which induces further
33
34 Ca^{2+} increments.

35
36
37
38
39
40
41
42
43 Although there is compelling evidence in the literature that Ca^{2+} is involved in ROS-
44
45 induced-MPTP opening in hepatocytes, there is no agreement as yet on the mechanisms
46
47 underlying this effect. A likely candidate to mediate Ca^{2+} -dependent mitochondrial damage
48
49 is calmodulin (CaM). This protein binds Ca^{2+} , and the complex is involved in a variety of
50
51 cell functions through the activation of CaM-dependent enzymes (Colbran 2004). CaM is
52
53 an ubiquitous protein found mainly in liver cytoplasm, nucleus, and plasma membrane
54
55 (Harper 1980), but mitochondria also contain CaM both on the inner membrane and in the
56
57 matrix space (Itano 1986). The organelle holds several CaM-binding proteins as well,
58
59
60
61
62
63
64
65

1
2
3
4 which have been implied as mediators of mitochondrial permeability transition (MPT) and
5
6 cell death. They include the phosphatase calcineurin (Molkentin 2001), the cysteine
7
8 protease calpain (Arrington 2006), and protein kinase Ca²⁺/calmodulin-dependent protein
9
10 kinase II (CaMKII) (Joiner 2012). Therefore, at least conceptually, Ca²⁺ overload occurring
11
12 under OS-conditions may excessively activate these CaM-downstream targets, leading to
13
14 MPTP opening and mitochondrial ROS generation.
15
16
17

18
19 In this work, we addressed this hypothesis by using *tert*-butyl hydroperoxide
20
21 (*t*BOOH) as a pro-oxidant compound. *t*BOOH is a synthetic analogue of short-chain lipid
22
23 hydroperoxides formed endogenously under OS conditions, which has been widely used as
24
25 a model to study the effect of OS on biological systems (Nieminen 1995; Byrne 1999;
26
27 Imberti 1993). Apart from inducing OS directly via reduction into both peroxy and alkoxy
28
29 free radicals by both cytochrome P450 and the mitochondrial electron chain (Davies 1989),
30
31 *t*BOOH promotes OS via ROS-induced MPTP formation and further mitochondrial
32
33 production of ROS. This is supported by the finding that MPTP blockers inhibit the late
34
35 phase of mitochondrial pyridine-nucleotide oxidation and ROS generation following
36
37 *t*BOOH exposure to isolated hepatocytes (Nieminen 1997). This makes *t*BOOH a unique
38
39 tool to study the factors regulating OS-dependent MPTP onset, and the further
40
41 hepatocellular death.
42
43
44
45
46
47
48
49
50
51
52
53
54
55
56
57
58
59
60
61
62
63
64
65

1
2
3
4
5
6
7
8
9

MATERIAL AND METHODS

10 **Materials.** Collagenase type A from Clostridium histolyticum was purchased from Gibco
11 (Paisley, UK). Leibovitz-15 (L-15) tissue culture medium, bovine serum albumin (fraction
12 V), *t*BOOH, dimethylsulphoxyde (DMSO), Triton X-100, EGTA, sodium dodecyl sulfate
13 (SDS), TEMED, DTT, leupeptin, urethane, PMSF, cyclosporin A (CsA), trifluorperazine
14 (TFP), FK-506 (tacrolimus), carbonyl cyanide *m*-chloro-phenylhydrazone (CCCP) and
15 tetramethylrhodamine methyl ester (TMRM) were from Sigma Chemical Co. (St. Louis,
16 MO). Cellular lysis buffer, KN-62, W7, mouse anti-CaMKII, and mouse anti rat phospho-
17 CaMKII were from Cell Signaling Technology (Beverly, MA). BAPTA/AM and Fura-
18 2/AM were from Molecular Probes (Eugene, Oregon, U.S.A.). Goat anti-mouse IgG
19 (#31430), chemiluminescence reagent, and Hyperfilm ECL were from Thermo Fisher
20 Scientific Inc. (Waltham, MA). All other chemicals were of reagent grade.
21
22
23
24
25
26
27
28
29
30
31
32
33
34
35
36
37
38
39

40 **Animals.** Adult male Wistar rats weighing 300-350 g were used throughout. Animals were
41 maintained on a standard diet and water ad libitum, and housed in a temperature (21°-23°
42 C) and humidity (45-50%) controlled room, under a constant 12-hour light, 12-hour dark
43 cycle. All animals received humane care, according to the Guide for the Care and Use of
44 Laboratory Animals prepared by the National Academy of Sciences and published by the
45 NIH (publication 25-28, revised 1996).
46
47
48
49
50
51
52
53
54
55
56
57

58 **Hepatocyte isolation.** Hepatocytes were isolated from livers by the collagenase perfusion
59
60
61
62
63
64
65

1
2
3
4 technique, using a modification of the method of Berry and Friend (Berry 1969). Briefly,
5
6 under urethane anesthesia (5mg/kg body wt, ip), heparin was administered in the inferior
7
8 vena cava (1.50 U/kg of body weight), and a 14G catheter (Abbocath-T, Venisystemtm,
9
10 Abbocath Ireland Ltd., Sligo, Ireland) was introduced in the portal vein. This was followed
11
12 by a 10-min, non-recirculant portal perfusion with a Ca²⁺-free, oxygenated (95% O₂/5%
13
14 CO₂) Hanks' solution, pH = 7.47-7.50, supplemented with HEPES (3 g/l) and EGTA (0.24
15
16 g/l). The livers were then perfused for a further 5-min period with the same solution
17
18 without EGTA, supplemented with 1 mM MgSO₄, 2.5 mM CaCl₂ and collagenase type IV
19
20 (430 U/l). Finally, the livers were removed, and the cells isolated by mechanical
21
22 dissociation by gently stirring with a glass stick for 3-4 min. Hepatocytes were further
23
24 purified from non-parenchymal cells by low-speed centrifugation (30xg, 2 min), followed
25
26 by 3 consecutive washings in oxygenated Hanks' solution containing 2.5 mM CaCl₂ and 5
27
28 mM Tris. The resulting preparation yielded ~ 400-600x10⁶ hepatocytes per liver, with high
29
30 viability (>90%), as assessed by the trypan blue exclusion test (Baur 1975).
31
32
33
34
35
36
37
38
39
40

41 ***Hepatocyte culture.*** Isolated hepatocytes were plated in 6-well plastic plates precoated with
42
43 rat tail collagen at least 1 day before preparing the hepatocyte cultures. Ice-cold neutralized
44
45 collagen solution was dispensed onto each dish/well, and the coated dishes/plates were
46
47 placed at 37° C in a humidified incubator for approximately 2 h to allow the matrix material
48
49 to gel, followed by addition of 3 ml of DMEM to each dish/plate and storage in a
50
51 humidified incubator. Hepatocyte suspensions were added to the precoated dishes/plates at
52
53 a density of 2 x 10⁶ cells/ 30mm dishes diluted in DMEM. Cells were allowed to attach for
54
55 2-2.5 h at 37° C in a air humidified atmosphere and 5 % CO₂. After attachment, the
56
57
58
59
60
61
62
63
64
65

1
2
3
4 medium was aspirated, and 3 ml of fresh DMEM was added.
5
6
7
8
9

10 **Treatments.** After 18 h of culture, hepatocytes were incubated with 500 μ M *t*BOOH (or the
11 vehicle, DMSO, in controls) for 15 min in a humidified incubator at 37° C, with 5% CO₂.
12
13 The effect of the pre-incubation of the hepatocytes with a number of modulators was
14 studied. Hepatocytes were pre-incubated with these modulators for 15 min, and then
15 exposed to *t*BOOH for a further 15-min period. The modulators were kept in the incubation
16 medium throughout *t*BOOH exposure.
17
18
19
20
21
22
23
24
25
26
27

28 **Evaluation of *t*BOOH effect on hepatocellular integrity.** At the end of the incubation
29 period with *t*BOOH, aliquots of hepatocytes were removed to assess cell viability, leakage
30 of the cytosolic enzyme, lactate dehydrogenase (LDH; EC 1.1.1.27), and ATP content.
31
32
33
34
35

36 Viability of hepatocytes cultured on multiwell plates was assessed by the trypan blue
37 exclusion test (Baur 1975).
38
39
40

41 Plasma membrane integrity was evaluated by the leakage of the cytosolic enzyme,
42 LDH, into the incubation medium. LDH activity was assessed spectrophotometrically
43 (Perkin Elmer UV/Vis Spectrometer Lambda2S, berlingen, Germany) by measuring NADH
44 consumption at 340 nm, using commercial kits (LDH-P UV AA liq, Wiener Lab., Rosario,
45 Argentina). LDH release (activity in the medium) was normalized to total LDH activity in
46 the cellular compartment. For this purpose, aliquots of the cellular suspension were treated
47 with Triton X-100 (0.1% v/v), followed by centrifugation at 9000xg for 2 min.
48
49
50
51
52
53
54
55
56
57

58 ATP content was measured using the substrate-enzyme system, luciferin-luciferase
59
60
61
62
63
64
65

1
2
3
4 (Lyman 1967).
5
6
7
8
9

10 **Evaluation of *tBOOH-induced OS*.** The magnitude of OS induced by *tBOOH* was
11 evaluated in hepatocytes cultured in precoated dishes by measuring generation of the lipid
12 peroxidation product malondialdehyde (MDA), and the oxidized glutathione (GSSG)-to-
13 total glutathione (GSht) ratio.
14
15
16
17
18

19
20 MDA was measured by reaction with thiobarbituric acid followed by the
21 fluorimetric HPLC detection of the MDA-thiobarbituric acid adduct formed, according to
22 the HPLC method of Fukunaga *et al.* (Fukunaga 1998). A standard curve using 1,1,3,3-
23 tetramethoxypropane, which is converted mol for mol into MDA, was routinely run.
24
25
26
27
28
29

30 Cell contents of GSht and GSSG were determined by the recycling method of Tietze
31 (Tietze 1969), as modified by Griffith (Griffith 1980).
32
33
34

35 Protein content in the aliquots of cell suspension used for the assay was measured by
36 the method of Lowry *et al.* (Lowry 1951), using BSA as a standard.
37
38
39
40
41
42

43 **Measurement of cytosolic Ca^{2+} concentration ($[Ca^{2+}]_i$).** $[Ca^{2+}]_i$ was assessed using Fura-
44 2/AM as a probe. For this purpose, 2×10^6 cells were suspended at 37° C in 3 ml of a PBS
45 (pH = 7.4) buffer solution containing 3 mM $CaCl_2$, and then supplemented with 1 μ M Fura-
46 2/AM. Fluorescence intensity (F) was measured by using alternating excitation
47 wavelengths of 340 and 380 nm, and a fluorescence emission wavelength of 510 nm (3 nm
48 bandwidth). $[Ca^{2+}]_i$ was calculated from the 340 nm/380 nm Fura-2/AM fluorescence
49 intensity ratio (R), according to the following equation (Grynkiewicz 1985):
50
51
52
53
54
55
56
57
58
59
60
61
62
63
64
65

1
2
3
4 $[Ca^{2+}]_i = K_d [(R-R_{min})/(R_{max}-R)] (F380_{min}/F380_{max})$
5
6

7 where K_d is the dissociation constant of the complex Fura-2/ Ca^{2+} (135 nM), R_{max} and R_{min}
8 are R values measured sequentially by addition of 10g/ml digitonin to the Fura-2-loaded
9 cells before and after chelating Ca^{2+} with 5 mM EGTA/Tris solution (pH = 8.7),
10 respectively.
11
12
13
14
15
16
17
18
19

20 **Assessment of MPTP formation.** MPTP generation was evaluated in primary culture of rat
21 hepatocytes by assessing the mitochondrial membrane potential as a surrogate marker,
22 using TMRM as a probe (Imberti 1993); TMRM is a membrane-permeable, cationic
23 fluorophore that accumulates electrophoretically in mitochondria in proportion to their
24 membrane potential ($\Delta\psi$). For this purpose, hepatocytes in 24-well plates were loaded at
25 37° C with 8 μ M TMRM in Krebs-Henseleit buffer for 10 min. The supernatant was then
26 aspirated to remove the excess of TMRM, and fluorescence intensity was measured using a
27 fluorescence multiwell plate reader using excitation and emission filters of 546 and 573 nm,
28 respectively. Mitochondrial $\Delta\psi$ was calculated from the 573 nm/546 nm TMRM
29 fluorescence intensity ratio (R), according to Scaduto and Grotyohann (Scaduto, Jr. 1999),
30 and expressed as the percentage of the change in mitochondrial depolarization, in a scale
31 ranging from a basal, non-depolarized condition (control value) to the maximal depolarized
32 condition, obtained by adding the respiratory chain uncoupling compound, CCCP (10 μ M).
33
34
35
36
37
38
39
40
41
42
43
44
45
46
47
48
49
50
51

52 Additionally, MPT was assessed in isolated mitochondria by monitoring the changes
53 in mitochondrial osmotic volume (swelling) secondary to MPTP formation. Swelling was
54 monitored by the decrease in apparent absorbance (light-scattering), since the light
55 scattered is inversely proportional to the mitochondrial volume (Azzone 1965). For this
56
57
58
59
60
61
62
63
64
65

1
2
3
4 purpose, the mitochondrial fraction (1 mg protein/ml) was resuspended in 1 ml of swelling
5
6 buffer composed of 5 mM KH_2PO_4 , 200 mM sucrose, 5 mM succinate (for mitochondria
7
8 energization), and 25 mM KCl (pH = 7.4). After a 2-min equilibration period, *t*BOOH (or
9
10 its vehicle, saline) was added so as reach a final concentration of 500 μM , and swelling was
11
12 monitored by recording the changes in absorbance at 540 nm with a Perkin Elmer Lambda
13
14 2S UV-Vis spectrophotometer computer controlled (Norwalk, USA).
15
16
17
18
19
20
21

22 ***Analysis of protein kinase activation.*** The activation of CaMKII and mitogen-activated
23
24 protein kinases (MAPKs) of the c-Jun NH2-terminal kinase 1/2 (JNK1/2) and p38^{MAPK}
25
26 types were assessed by Western blotting using a antibodies recognizing the activate forms
27
28 of these kinases, which are phosphorylated at Thr²⁸⁶, Thr¹⁸³/Tyr185, and Thr¹⁸⁰/Tyr¹⁸²,
29
30 respectively.
31
32
33
34

35 For this purpose, the content of phosphorylated and total forms of the proteins was
36
37 analyzed by Western blotting of primary hepatocyte cultures. After treatment, hepatocytes
38
39 were washed with cold PBS and resuspended in a cellular lysis buffer containing protease
40
41 inhibitors (leupeptin 25 g/ml and PMSF 0.1 mM). Aliquots containing equivalent total
42
43 protein content were subjected to SDS, 12% polyacrylamide gel electrophoresis. Separated
44
45 proteins were electrotransferred to PVDF membranes, and probed overnight with anti-
46
47 phospho-CaMKII (1:2000), anti-phospho-JNK1/2 antibody (1:2000), or anti-phospho-
48
49 p38^{MAPK} (1:300) antibodies. Membranes were then stripped, and reprobed with an anti total-
50
51 CaMKII (1:2000), anti-total JNK1/2 (1:5000), or anti-total p38^{MAPK} (1:500) antibodies.
52
53
54 After using a goat anti-mouse or a mouse anti-goat IgG secondary antibody (1:5000)
55
56 depending on the primary antibody used, a chemiluminescence reagent, and Hyperfilm
57
58
59
60
61
62
63
64
65

1
2
3
4 ECL, the phospho and total bands of each studied protein were quantified by densitometry
5
6 using the Image J 1.34m software.
7
8
9

10
11
12 ***Apoptosis analysis.*** Apoptosis was evaluated by the Annexin V/ propidium iodide (PI) flow
13
14 cytometry assay (Vermes 1995). In addition, the involvement of the mitochondrial
15
16 apoptosis pathway in *t*BOOH-induced hepatocellular death was studied by assessing
17
18 mitochondrial cytochrome *c* release into cytosol, the subsequent increase in caspase-3
19
20 activity, and the balance between proapoptotic (Bax) and antiapoptotic (Bcl-xL)
21
22 mitochondrial proteins.
23
24
25

26
27 ***Annexin V flow cytometry assay.*** After gently homogenization in the culture medium/PBS
28
29 and harvest (5 min, 400 g), hepatocytes were carefully re-suspended in the appropriate
30
31 buffer at the desired concentration. Apoptotic externalization of phosphatidylserine and cell
32
33 death in hepatocytes was assessed by staining with Annexin V-FITC and PI (Annexin V-
34
35 FITC Apoptosis Detection Kit, Sigma Chemical Co, St Louis, MO), respectively, coupled
36
37 to flow cytometric analysis (Cell Sorter BD FACSAria II, Becton, Dickinson and Co,
38
39 Franklin Lakes, NJ), following the manufacturer's instructions. Detection of green and red
40
41 fluorescence was carried out; green and red fluorescence intensities detected in non stained
42
43 cells were used to set the thresholds for each channel. Annexin V positive cells, irrespective
44
45 of whether they were PI positive or negative cells, were considered to be apoptotic in
46
47 nature, either at an early stage of apoptosis (annexin V positive/PI negative cells) or at an
48
49 late stage of apoptosis (annexin V positive/PI positive cells). Even when necrotic cells all
50
51 share the same features as late stage apoptotic cells in terms of pattern of annexin
52
53 V/propidium iodide staining, necrosis can be ruled out from our results showing conserved
54
55
56
57
58
59
60
61
62
63
64
65

1
2
3
4 ATP cellular content (Table 1). Indeed, for the occurrence of apoptosis, normal levels of
5
6 ATP are necessary, whereas low cellular ATP levels are indicative of necrosis (Eguchi
7
8 1997).
9

10
11 *Immunoblot analysis of pro- and anti-apoptotic proteins.* The levels of cytochrome *c* (in
12
13 cytosol) and of Bax and Bcl-xL (mitochondria), all proteins involved in the apoptosis
14
15 process, was determined by immunoblotting. Cytosolic and mitochondrial fractions were
16
17 prepared by differential centrifugation, as previously described (Kim 2006). Briefly,
18
19 mitochondria-enriched fractions were prepared from hepatocytes that were homogenized in
20
21 sacarose 0.3 M with protease inhibitors (1 mM phenylmethylsulfonyl fluoride, 10 mg/ml
22
23 leupeptin, and 1 mg/ml aprotinin), and sonicated. Homogenates were centrifuged at 1000xg
24
25 to remove unbroken cells, nuclei, and heavy membranes. Mitochondria enriched fractions
26
27 were then obtained by the centrifugation of supernatant at 6000xg at 4°C for 15 min. Then,
28
29 the supernatant was centrifuged at 45000xg for 1 h to obtain the cytosolic fraction (Ronco
30
31 2004). Proteins were quantified in these fractions according to Lowry *et al.* (LOWRY
32
33 1951). For immunoblotting, 20 µg of protein were subjected to 12% SDS-PAGE, and
34
35 transferred to Immobilon polyvinylidene difluoride (PVDF) membranes (Perkin Elmer Life
36
37 Sciences, Boston, MA, USA). Membranes were blocked with 5% non-fat milk/0.3%
38
39 Tween/PBS, washed, and incubated overnight at 4 °C with a specific primary antibody
40
41 against Bax, Bcl-xL, or cytochrome *c* (1:600, Santa Cruz Biotechnology, Santa Cruz, CA,
42
43 USA). Then, membranes were incubated with the appropriate secondary antibody
44
45 conjugated with horseradish peroxidase (1:5000, Amersham Life Science), and the
46
47 resulting bands were detected by enhanced chemiluminescence (ECL; Amersham
48
49 Pharmacia Biotech). Autoradiographs were obtained by exposing PVDF membranes to
50
51
52
53
54
55
56
57
58
59
60
61
62
63
64
65

1
2
3
4 Amersham hyperfilm™ ECL (GE Healthcare), and the bands quantified by densitometry
5
6 using the Gel-Pro Analyzer software (Media Cybernetics, Silver Spring, MD).
7
8
9

10
11
12 *Assessment of caspase-3 activity.* Caspase-3 activity was determined according to the
13 manufacturer's instructions, using an EnzChek caspase-3 assay kit (Molecular Probes,
14 Eugene, OR, USA). The tissues were homogenized in lysis buffer (10 mM Tris, 200 mM
15 NaCl, 1 mM EDTA, and 0.001% Triton X-100). After differential centrifugation, the
16 cytosolic fraction from each sample was mixed with a Z-Asp-Glu-Val-Asp-AMC substrate
17 solution. A standard curve of AMC ranging from 0-100 mM was run. A control sample
18 without enzyme was used to determine the background fluorescence of the substrate.
19
20 Fluorescence was measured at an excitation wavelength of 360 nm and an emission
21 wavelength of 465 nm in a DTX 880 Multimode Detector (Beckman Coulter, Brea, CA,
22 USA).
23
24
25
26
27
28
29
30
31
32
33
34
35
36
37
38
39

40 *Statistical analysis.* Data are expressed as mean \pm SE. Multiple means were compared with
41 one-way ANOVA followed by Tukey's test for pairwise comparisons, by using a computer
42 program (PHARM/PCS, MicroComputer Specialist, Philadelphia). Differences were
43 considered significant when the p values were < 0.05 .
44
45
46
47
48
49
50
51
52
53
54
55
56
57
58
59
60
61
62
63
64
65

RESULTS

Characterization of tBOOH-induced impairment in hepatocellular integrity, oxidative stress generation, changes in ATP content and cytosolic Ca²⁺ elevations. As shown in Table 1, tBOOH (500 μM, 15 min) impaired hepatocellular integrity, as indicated by a 38% decrease in cell viability, and a 31% increase in the release to the incubation medium of the cytosolic enzyme, LDH. Contrarily, ATP content was not affected by the oxidant agent.

An increase in ROS levels was clearly apparent after tBOOH exposure, as indicated by the enhancement of one order of magnitude in the generation of the lipid peroxide malondialdehyde (Table 1); this was associated with a decrease in both total (GSH + GSSG) glutathione and the GSSG-to-total glutathione ratio. This OS was instrumental in increasing dramatically (by ~25 times) the cytosolic, free Ca²⁺ concentration.

Effect of intracellular Ca²⁺ sequestration and CaM/CaMKII inhibition on tBOOH-induced changes in mitochondrial Δψ and lipid peroxidation (LPO). MPTP formation induced by tBOOH was assessed by measuring depolarization of mitochondrial Δψ as a surrogate parameter, using the mitochondrial-sensitive cation TMRM as a probe. The dependency of mitochondrial Δψ on MPTP formation was corroborated by our own result that the MPTP blocker CsA diminished significantly the changes in mitochondrial Δψ induced by tBOOH (Fig. 1, A); the difference between the changes in mitochondrial Δψ induced by tBOOH and the changes of this parameter in the presence of CsA can be thus regarded as a measure of MPTP formation.

1
2
3
4 The degree of LPO, as measured by MDA content, was dramatically increased by
5
6 *t*BOOH, and the MPTP blocker CsA inhibited partially this effect (Fig. 1, *B*); a similar
7
8 phenomenon had been reported elsewhere using the OS-sensitive fluorescent dye
9
10 dichlorofluorescein as a probe to assess ROS generation (Nieminen 1997). This support the
11
12 contention that *t*BOOH capability to induce ROS depends not only on the generation of
13
14 peroxy- and alkoxy-free radicals after metabolization (Davies 1989) but also on its
15
16 capability to induce MPTP formation. This CsA-sensitive fraction of *t*BOOH-induced LPO
17
18 provides an observational window where the influence of signaling modulators on OS from
19
20 mitochondrial origin can be monitored.
21
22
23
24

25
26 As can be also seen in Fig. 1 *A* and *B*, the intracellular Ca²⁺-sequestering agent
27
28 BAPTA/AM attenuated *t*BOOH-induced both mitochondrial depolarization and LPO to a
29
30 similar extent to CsA. Overall, these results indicate that *t*BOOH-induced LPO depends
31
32 partially on MPTP generation, and that this effect is facilitated by intracellular Ca²⁺
33
34 elevations.
35
36
37
38

39 In an attempt to find it out possible mediators of the facilitating effect of Ca²⁺ on
40
41 MPTP formation and the further generation of mitochondrial ROS, we assessed the
42
43 involvement of CaM and two of its putative downstream mediators, CaMKII and
44
45 calcineurin, in the capability of *t*BOOH to induce MPT and LPO of mitochondrial origin.
46
47 As shown in Fig. 1 *A* and *B*, respectively, the CaM antagonists TFP and W7 prevented
48
49 completely the CsA-sensitive changes in mitochondrial $\Delta\psi$ and MDA content induced by
50
51 *t*BOOH; CsA effect was not additive with that of W7, strongly suggesting that both the
52
53 MPTP blocker and the CaM inhibitor acts via a similar mechanism, *i.e.* inhibition of MPTP
54
55 formation. Similarly to the CaM inhibitors, the specific CaMKII inhibitor KN-62, but not
56
57
58
59
60
61
62
63
64
65

1
2
3
4 the calcineurin inhibitor FK-506 (tacrolimus), fully prevented both alterations. This
5
6 indicates that both the onset of MPTP induced by *t*BOOH and the resulting oxidative stress
7
8 from mitochondrial origin are modulated by CaM, via CaMKII activation.
9

10
11
12
13
14
15 ***Effect of tBOOH on CaMKII activation.*** Western blot analysis of phosphorylated CaMKII
16
17 showed that the amount of the phosphorylated, active form of CaMKII significantly
18
19 increased at 15 min after *t*BOOH administration (Fig. 2). On the other hand, total CaMKII
20
21 content remained unchanged. Pretreatment with the CaM inhibitors TFP and W7, or with
22
23 the CaMKII inhibitor KN-62, completely prevented the increase in phosphorylated
24
25 CaMKII. This rules out the alternative possibility that CaMKII is activated by direct
26
27 oxidation of paired methionine residues in the regulatory domain of CaMKII in the absence
28
29 of Ca²⁺/CaM, as was shown to occur in cardiomyocytes (Erickson 2008).
30
31
32
33
34
35
36

37 ***Effect of tBOOH on JNK1/2 and p38^{MAPK} activation.*** Western blot analysis of
38
39 phosphorylated and total forms of JNK1/2 and p38 MAPK showed that the amount of the
40
41 phosphorylated, active form of these MAPKs significantly increased at 15 min of *t*BOOH
42
43 administration, whereas total JNK1/2 and p38^{MAPK} content remained unchanged (Fig. 3).
44
45 Pretreatment with the Ca²⁺-chelating agent BAPTA/AM, the CaM inhibitors TFP and W7,
46
47 or with the CaMKII inhibitor KN-62 completely prevented the increase in phosphorylated
48
49 JNK1/2 and p38^{MAPK}.
50
51
52
53
54
55
56

57 ***tBOOH induces apoptosis via the Ca²⁺/CaM/CaMKII signaling pathway.*** Because
58
59 dissipation of the mitochondrial potential is a common and early feature of apoptosis, we
60
61

1
2
3
4 analyzed here whether *t*BOOH exposure leads to apoptosis, and whether inhibition of the
5
6 $\text{Ca}^{2+}/\text{CaM}/\text{CaMKII}$ signaling pathway at different steps prevents this effect. Cytometric
7
8 annexin V/propidium iodide assay showed that *t*BOOH significantly increased annexin V
9
10 (+) /propidium iodide (-) cells (early apoptosis) by 86% (Fig. 4, A). The proportion of
11
12 annexin V (+)/propidium iodide (+) (late apoptosis) also was increased by 122% (Fig. 4, B).
13
14 As a consequence, the proportion of cells with either early or late apoptosis, *i.e.*, annexin V
15
16 (+) cells, was increased by 89% by *t*BOOH (Fig. 5, C). On the other hand, in cell pretreated
17
18 with inhibitors acting at different levels in the $\text{Ca}^{2+}/\text{CaM}/\text{CaMKII}$ signaling pathway, the
19
20 proportion of cells with either early apoptosis or late apoptosis after *t*BOOH exposure was
21
22 similar to that of control cells, or to that treated with the MPTP blocker CsA (Fig. 4, A and
23
24 B, respectively). A similar pattern of prevention was obtained when the proportion of
25
26 apoptotic cells irrespective of their stage was considered (Fig. 4, C).
27
28
29
30
31
32
33
34
35

36 ***Involvement of the mitochondrial pathway in tBOOH-induced apoptosis.*** The role for
37
38 mitochondria in *t*BOOH-induced apoptosis via the $\text{Ca}^{2+}/\text{CaM}/\text{CaMKII}$ signaling pathway
39
40 was assessed by studying the release of mitochondrial cytochrome *c* into cytosol, the
41
42 further increase in the activity of caspase-3, and the balance between the mitochondrial pro-
43
44 apoptotic protein Bax and the anti-apoptotic protein Bcl-xL.
45
46
47
48

49 Immunoblot analysis of cytosolic cytochrome *c* showed that there was an increase of
50
51 ~120% in cytochrome *c* release from mitochondria after *t*BOOH exposure, and that Ca^{2+}
52
53 sequestration with BAPTA, inhibition of CaM with TFP or W7, and CaMKII inhibition
54
55 with KN-62 all fully prevented mitochondrial cytochrome *c* release (Fig. 5).
56
57
58

59 As anticipated from the fact that cytosolic cytochrome *c* triggers apoptosis via
60
61

1
2
3
4 activation of the executioner caspase-3, the activity of this caspase increased approx. 3 times
5
6 in cytosol after *t*BOOH exposure. This effect was also fully prevented by the MPTP
7
8 blocker CsA, indicating that the “intrinsic” (mitochondrion-driven) pathway of caspase-3
9
10 activation is triggered by *t*BOOH (Fig. 6). Ca²⁺ sequestration with BAPTA, inhibition of
11
12 CaM with TFP or W7, and CaMKII inhibition with KN-62 all fully prevented the increase
13
14 in caspase-3 activity at the same extent as CsA did.
15
16
17
18

19
20 Finally, we examined the expression of Bax and Bcl-xL at the protein level in the
21
22 mitochondrial fraction by western blot analysis. Bax and Bcl-xL are members of the Bcl-2
23
24 family which plays major, opposite roles as regulators of the apoptotic process: while Bax
25
26 acts as a promoter, Bcl-xL acts as an inhibitor (Tzung 1997). Immunoblot analyses revealed
27
28 that mitochondrial Bax protein levels increased by 139% (P < 0.01) after *t*BOOH
29
30 administration, whereas Bcl-xL remained virtually unchanged (Fig. 7, *upper panel*).
31
32 Consequently, Bax-to-Bcl-xL ratio, an indicator of cell vulnerability to apoptosis, was
33
34 increased by 186% by *t*BOOH (Fig. 7, *lower panel*). Inhibition of CaM with TFP or W7,
35
36 and inhibition of CaMKII with KN-62 both prevented the increase in both Bax
37
38 mitochondrial level and Bax-to-Bcl-xL ratio.
39
40
41
42
43
44

45
46 ***Involvement of mitochondrial CaMKII in tBOOH-induced MPTP.*** CaMKII is a
47
48 ubiquitous enzyme, and CaMKII with mitochondrial localization has been recently reported
49
50 to play a crucial role in Ca²⁺-induced MPTP and apoptosis in cardiomyocytes (Joiner
51
52 2012). To assess the involvement of mitochondrion-localized CaMKII in *t*BOOH-induced
53
54 MPTP formation in hepatocytes, we studied in isolated hepatocellular mitochondria the
55
56 effect CaMKII on *t*BOOH-induced osmotic swelling of the mitochondrial matrix, a
57
58
59
60
61
62
63
64
65

1
2
3
4 phenomenon due to opening of MPTPs in the inner mitochondrial membrane. The time
5
6 course of mitochondrial swelling, as monitored by recording the decrease in absorbance
7
8 (light-scattering) at 540 nm over 15 min, is shown in Fig. 8. Control mitochondria treated
9
10 with the *t*BOOH vehicle showed a slight decrease due to spontaneous swelling, whose
11
12 magnitude agrees with results obtained by others (Roy 2009; Lee 2008). On the other hand,
13
14 *t*BOOH induced a fast decrease in light scattering due to MPTP formation, as confirmed by
15
16 the fact that the MPTP blocker CsA fully abrogated this effect. Swelling was less
17
18 pronounced when either the CaM inhibitor W7 or the CaMKII inhibitor KN-62 was present
19
20 in the medium, suggesting a partial role for a mitochondrial Ca²⁺/CaM/CaMKII signalling
21
22 pathway in *t*BOOH-mediated effect.
23
24
25
26
27
28
29
30
31
32
33
34
35
36
37
38
39
40
41
42
43
44
45
46
47
48
49
50
51
52
53
54
55
56
57
58
59
60
61
62
63
64
65

DISCUSSION

MPTP onset has been implicated as a pivotal event contributing to hepatocyte cell death under OS conditions. This was readily apparent from studies showing that MPTP blockers inhibit the late phase of mitochondrial pyridine nucleotide oxidation and ROS generation in isolated hepatocytes exposed to *t*BOOH (Nieminen 1997). The MPTPs generated by an initial oxidant insult (ROS generated from *t*BOOH metabolization, in our case) further exacerbate ROS production by inducing leakage of electrons from the mitochondrial respiratory chain, which triggers a detrimental vicious circle (Nieminen 1995).

Despite there is compelling evidence in the literature that Ca^{2+} is involved in MPTP onset caused by oxidizing agents in hepatocytes (Imberti 1993; Byrne 1999), the intracellular events mediating this effect has not been fully clarified as yet; its elucidation is however relevant to develop new therapeutic approaches for protection against OS-induced hepatocellular damage. In this report, we provide novel evidence that the Ca^{2+} /CaM/CaMKII signaling pathway plays a pivotal role in both *t*BOOH-induced MPTP formation in hepatocytes and its potential to exacerbate OS from mitochondrial origin, two events that are linked causally with each other. This is supported by our finding that Ca^{2+} sequestration with BAPTA, blockage of the formation of the Ca^{2+} /CaM complex with W7 or TFP, or inhibition of CaMKII with KN-62 all prevented *t*BOOH-induced OS and MPTP formation to a similar extent to the MPTP blocker CsA (see Fig. 1). Our finding that no additive effect was recorded when both MPTP and CaM were simultaneously inhibited by CsA and W7, respectively (see Fig. 1), further confirms the involvement of MPTP as a common target of both inhibitors.

1
2
3
4 Disruption of intracellular Ca^{2+} homeostasis and defects in mitochondrial function
5
6 induce cell death in a variety of pathological conditions involving Ca^{2+} elevations and
7
8 oxidative damage [for reviews, see (Orrenius 1992; Lemasters 2009)]. Several lines of
9
10 evidence indicate that many of these detrimental effects are mediated by CaM and/or
11
12 CaMKII. For example, CaM and CaMKII inhibitors protect against both
13
14 hypoxia/hypoglycemia- (Hajimohammadreza 1995) and veratridine-induced neuronal
15
16 depolarization (Takano 2003). In addition, CaM antagonists attenuate MPTP-mediated
17
18 neuronal death due to ischemia (Kuroda 1997), and apoptotic death of pheochromocytoma
19
20 cells (PC12) induced by the depolarizing agent 1-methyl-4-phenylpyridinium (Lee 2005).
21
22 In the latter cell line, ROS formation, cytochrome *c* release, activation of caspase-3 and cell
23
24 death induced by rotenone, an inhibitor of mitochondrial-respiratory-chain-complex I, was
25
26 counteracted by CaM antagonists. Similarly, CaM antagonists protected rat heart
27
28 myocardium H9c2 cells against toxicity of rotenone by suppressing ROS formation
29
30 (Yaglom 2003). Moreover, in rat ventricular, permeabilized cardiomyocytes, direct CaM
31
32 exposure induced depolarization of $\Delta\psi$ mitochondrial and opening of MPTP by increasing
33
34 ROS production in a CaMKII-dependent manner (Odagiri 2009) Finally, CaMKII has been
35
36 implied in cadmium-induced apoptosis in mesangial cells (Liu 2007).
37
38
39
40
41
42
43
44

45
46 The role of Ca^{2+} /CaM/CaMKII signaling pathway in MPTP opening and the
47
48 associated generation of OS from mitochondrial origin had not been assessed in
49
50 hepatocytes. Only some reports provides circumstantial evidence that CaM and/or CaMKII
51
52 are involved in ROS generation and OS-induced liver damage, such as that induced by the
53
54 hepatotoxicants acetaminophen (Dimova 1995) and CCl_4 (Villarruel 1990). However, the
55
56 action mechanisms of these toxic compounds are multifactorial in nature, and this prevents
57
58
59
60
61
62
63
64
65

1
2
3
4 a clear conclusion to be drawn on the CaM and/or CaMKII mechanisms of action. In this
5
6 work, we provide mechanistic support for these preliminary results by showing that CaM
7
8 modulates OS from mitochondrial origin via MPTP formation and further apoptotic
9
10 hepatocellular death, and that this effect involves CaMKII as a main downstream effector.
11
12

13
14 CaMKII belongs to the multifunctional, Ca²⁺/CaM-activated, serine/threonine kinase
15
16 family (Hudmon 2002). Therefore, CaMKII may influence MPTP onset by modifying the
17
18 phosphorylation status of mitochondrial proteins belonging to, or regulating, MPTP. In line
19
20 with this, changes in the phosphorylation status of several low-molecular-weight,
21
22 mitochondrial proteins were observed in rat brain associated with MPTP opening.
23
24 Interestingly, this phenomenon was dependent on Ca²⁺, and prevented by the CaM
25
26 antagonist calmidazolium (Azarashvili 2003).
27
28
29
30

31
32 It is difficult at this stage to identify specific putative structural or regulatory
33
34 components of the MPTP as target for CaMKII-mediated phosphorylation. To the best of
35
36 our knowledge, only VDAC has been described to be regulated by different kinases, such
37
38 as PKA (Bera 2001) and PKCε (Baines 2003), but all these phosphorylations inhibited
39
40 rather than enhanced MPTP opening probability. Finally, the “novel” PKC isoform PKCδ
41
42 travels to mitochondria under OS conditions, where it triggers the release of cytochrome *c*
43
44 and apoptosis (Horbinski 2005; Majumder 2001). However, this member of the “novel”
45
46 PKC family is unresponsive to Ca²⁺. Alternatively, the “conventional”, Ca²⁺-dependent
47
48 PKC isoform PKCα, which we had showed to be activated by *t*BOOH in a previous work
49
50 even at lower concentrations (100 μM) (Perez 2006), has prosurvival rather than
51
52 proapoptotic functions in several cell lines (Horbinski 2005; Ruvolo 1998). Lack of
53
54 involvement of all these PKC isoforms was further confirmed by our results that neither
55
56
57
58
59
60
61
62
63
64
65

1
2
3
4 phorbol-12-myristate 13-acetate nor staurosporine, which activates and inhibits both
5
6 “conventional” and “novel” PKC isoforms, respectively (Gschwendt 1996), modified
7
8 *t*BOOH capability to induce ROS generation, MPTP onset and apoptosis (data not shown).
9

10
11
12 Rather, our results are more consistent with the existence of signaling cascades
13
14 downstream of CaMKII involving JNK and p38^{MAPK} (see Fig. 3). This finding is in line
15
16 with previous results showing that CaMKII can phosphorylate and activate both p38^{MAPK}
17
18 (Nguyen 2004) and JNK1/2 (Brnjic 2010), and that this event leads to apoptosis via
19
20 activation of the upstream protein *apoptosis signal-regulating kinase 1* (ASK1) (Brnjic
21
22 2010; Liu 2013). A rol for these MAPKs in *t*BOOH-induced MPTP opening by
23
24 phosphorylating apoptosis-related mitochondrial proteins is indeed likely. p38^{MAPK}
25
26 phosphorylates VDAC in myocytes after myocardial ischemia reperfusion, and the
27
28 kinase inhibition counteracted necrosis induced by this manoeuvre (Schwartz 2007);
29
30 unfortunately, MPTP generation was not assessed under this condition. As for JNK, its
31
32 activation has been shown to trigger Bax translocation to mitochondria by phosphorylation
33
34 of the Bax cytosolic anchor protein 14-3-3 (Tsuruta 2004); this may explain our finding that
35
36 mitochondrial Bax content increases after *t*BOOH exposure in a Ca²⁺/CaM/CaMKII-
37
38 dependent manner (see Fig. 7). Once in mitochondria, Bax oligomerizes in the outer
39
40 mitochondrial membrane to form pores, which allows for cytochrome *c* release and further
41
42 caspase-3 activation (Orrenius 2007), two events that have been also shown to occur here
43
44 after *t*BOOH exposure in a Ca²⁺/CaM/CaMKII-dependent manner (see Figs. 5 and 6,
45
46 respectively). The alternative possibility that JNK regulates Bax by direct phosphorylation
47
48 is also likely. In the human hepatoma cell line HepG2, various cell death agonists,
49
50 including pro-oxidant ones, induced apoptosis by promoting mitochondrial Bax
51
52
53
54
55
56
57
58
59
60
61
62
63
64
65

1
2
3
4 translocation via its phosphorylation at Thr¹⁶⁷ by both JNK and p38^{MAPK} (Kim 2006).
5
6 Whether activation of these kinases explains the dependency of *t*BOOH-induced apoptosis
7
8 on CaMKII activity remains to be ascertained, and this is the subject of ongoing research.
9
10 The possibility is likely, since CaMKII-dependent activation of JNK has been demonstrated
11
12 to occur in other cellular models leading to mitochondrion-driven apoptosis (Timmins
13
14 2009; Li 2012).
15
16
17
18

19 Alternatively, CaMKII may upregulate by phosphorylation the activity of a
20
21 phosphatase able to activate by dephosphorylation the effects of pro-apoptotic proteins
22
23 known to be inhibited the phosphorylating activity of other protein kinases. For example,
24
25 calcineurin, a Ca²⁺/CaM-dependent, serine-threonine phosphatase, induces apoptosis by
26
27 promoting Bad dephosphorylation (Wang 1999). However, we were unable to abrogate
28
29 *t*BOOH-induced both LPO and changes in mitochondrial $\Delta\psi$ by pre-treating hepatocytes
30
31 with FK506, a specific calcineurin inhibitor (see Fig. 1). Incidentally, the lack of effect of
32
33 FK506 confirms that the protective effect of CsA reported here was not due to its well-
34
35 establish inhibitory effect on calcineurin phosphatase activity (Hemenway 1999), but to its
36
37 capability to abrogate MPTP onset (Bernardi 1996).
38
39
40
41
42
43

44 Another possibility, which may well act in concert with the previous ones, is that
45
46 CaMKII increases primarily mitochondrial Ca²⁺ uptake, and that the increase in
47
48 mitochondrial Ca²⁺ helps *per se* to trigger MPTP opening by potentiating the capability of
49
50 ROS to onset MPTP (Byrne 1999; Vercesi 2006). In line with this, a tight temporal
51
52 correlation has been shown to exist between the increase in mitochondrial Ca²⁺ levels
53
54 induced by *t*BOOH and the opening of MPTPs in primary cultured hepatocytes (Byrne
55
56 1999). This holds true for other cell lines as well. In permeabilized rat ventricular
57
58
59
60
61
62
63
64
65

1
2
3
4 myocytes, exogenously added CaM opens MPTPs in a CaMKII-dependent manner, and this
5
6 effect was causally related to the uptake of Ca²⁺ released from sarcoplasmic reticulum by
7
8 neighboring mitochondria (Odagiri 2009). Complementarily, CaMKII mediates increase in
9
10 Ca²⁺ entry through the inner membrane of the cardiomyocytes mitochondria via the
11
12 mitochondrial Ca²⁺ uniporter (Joiner 2012). Furthermore, exogenously administered CaM
13
14 stimulated ROS production in the mitochondrial matrix of cardiomyocytes in part via
15
16 MPTP formation (Odagiri 2009). Recent studies by another group demonstrated that
17
18 mitochondrial rather than cytosolic CaMKII isoform is involved in CaM capability to open
19
20 MPTPs in this cell type, since mitochondrial targeting of a CaMKII inhibitor fully
21
22 abrogated this effect (Joiner 2012). However, our results in hepatocyte isolated
23
24 mitochondria showing that the CaM inhibitor W7 and the CaMKII antagonist KN-62
25
26 inhibited *t*BOOH-induced MPTP formation only *partially* (see Fig. 8) suggest that cytosol-
27
28 localized CaMKII cooperates with the mitochondrial one to account for the *full* mediation
29
30 of this enzyme in the MPTP opening recorded in intact hepatocytes (see Fig. 1).
31
32
33
34
35
36
37

38
39 Another important Ca²⁺-mediated intramitochondrial mechanism involved in *t*BOOH-
40
41 mediated MPTP formation is the activation of the Ca²⁺-dependent cysteine protease
42
43 calpain. Selective inhibition of this protease was shown to *fully* abrogate *t*BOOH-induced
44
45 MPTP onset in isolated rat mitochondria (Aguilar 1996); the absolute dependency of MPTP
46
47 formation on calpain activity suggests that CaMKII and calpain act through a common
48
49 mechanism to onset MPTP. There is some circumstantial evidence in the literature that
50
51 CaMKII can phosphorylate and activate calpain, as has been shown for calpain II isolated
52
53 from vascular smooth muscle (McClelland 1994). The reverse activation sequence also may
54
55 occur, since calpain I, like other proteases including caspases, activates *in vitro*
56
57
58
59
60
61
62
63
64
65

1
2
3
4 autophosphorylated CaMKII by proteolysis (Rich 1990). Whether this mutual activation
5
6 applies to mitochondrial calpain isoform/s remains to be ascertained. Alternatively,
7
8 CaMKII-mediated phosphorylation of a protein involved in MPTP formation may sensitize
9
10 this substrate for further calpain-dependent proteolysis, as was described for the calpain-
11
12 induced proteolytic cleavage of GluR1 C-terminal fusion protein in cortical neurons (Yuen
13
14 2007). Irrespective of the mechanism involved, a similar common dependency on CaMKII
15
16 and calpain activity to produce cell death has been identified in another apoptosis model in
17
18 hepatocytes, such as that induced by the protein phosphatase inhibitor microcystin (Ding
19
20 2002). Actually, the *t*BOOH pro-apoptotic mechanisms revealed here strongly resembles
21
22 those of microcystin in hepatocytes. In the case of microcystin, CaMKII is activated *before*
23
24 ROS formation via inhibition of its dephosphorylation, and activated CaMKII mediates
25
26 ROS mitochondrial formation via MPTP opening and further cytochrome *c* release, which
27
28 triggers the execution of apoptosis (Ding 2003). Our results here showing that a similar
29
30 mechanism applies for a “pure” model of OS strongly contributes to extrapolate this
31
32 concept to other pro-oxidant hepatotoxicants, and to the several pathological situations
33
34 involving OS as a cause of apoptotic hepatocellular death.
35
36
37
38
39
40
41
42

43
44 In summary, as schematized in Fig. 9, our study shows that the $\text{Ca}^{2+}/\text{CaM}/\text{CaMKII}$
45
46 pathway plays a major role in *t*BOOH-induced MPTP formation, and the consequent
47
48 exacerbation of both ROS formation from mitochondrial origin and hepatocellular
49
50 apoptosis. This points CaM and CaMKII as promising targets for the development of new
51
52 therapies to counteract hepatocellular oxidative damage.
53
54
55
56
57
58
59
60
61
62
63
64
65

1
2
3
4
5
6
7
8
9
10
11
12
13
14
15
16
17
18
19
20
21
22
23
24
25
26
27
28
29
30
31
32
33
34
35
36
37
38
39
40
41
42
43
44
45
46
47
48
49
50
51
52
53
54
55
56
57
58
59
60
61
62
63
64
65

Acknowledgments. This work was supported by grants from Agencia Nacional de Promoción Científica y Tecnológica (PICT 2010-0992), and Consejo Nacional de Investigaciones Científicas y Técnicas (PIP 112-200801-00691). We thank Justina Elena Ochoa, Diego Taborda, and Mara Ojeda for their valuable technical assistance.

Conflict of interest statement The authors declare that they have no conflict of interest

REFERENCES

- Aguilar HI, Botla R, Arora AS, Bronk SF, Gores GJ (1996) Induction of the mitochondrial permeability transition by protease activity in rats: a mechanism of hepatocyte necrosis. *Gastroenterology* 110:558-566. doi: 10.1053/gast.1996.v110.pm8566604
- Arrington DD, Van Vleet TR, Schnellmann RG (2006) Calpain 10: a mitochondrial calpain and its role in calcium-induced mitochondrial dysfunction. *Am J Physiol Cell Physiol* 291:C1159-C1171. doi: 10.1152/ajpcell.00207.2006
- Azarashvili T, Krestinina O, Odinkova I, Evtodienko Y, Reiser G (2003) Physiological Ca^{2+} level and Ca^{2+} -induced permeability transition pore control protein phosphorylation in rat brain mitochondria. *Cell Calcium* 34:253-259. doi: 10.1016/S0143-4160(03)00107-6
- Azzone GF, Azzi A (1965) Volume changes in liver mitochondria. *Proc Natl Acad Sci USA* 53:1084-1089. doi: 10.1073/pnas.53.5.1084
- Baines CP, Song CX, Zheng YT, Wang GW, Zhang Jet al. (2003) Protein kinase Cepsilon interacts with and inhibits the permeability transition pore in cardiac mitochondria. *Circ Res* 92:873-880. doi: 10.1161/01.RES.0000069215.36389.8D
- Baur H, Kasperek S, Pfaff E (1975) Criteria of viability of isolated liver cells. *Hoppe Seylers Z Physiol Chem* 356:827-838. doi: 10.1515/bchm2.1975.356.s1.827
- Bera AK, Ghosh S (2001) Dual mode of gating of voltage-dependent anion channel as revealed by phosphorylation. *J Struct Biol* 135:67-72. doi: 10.1006/jsbi.2001.4399
- Bernardi P (1996) The permeability transition pore. Control points of a cyclosporin A-sensitive mitochondrial channel involved in cell death. *Biochim Biophys Acta* 1275:5-9. doi: 10.1016/0005-2728(96)00041-2
- Berry MN, Friend DS (1969) High-yield preparation of isolated rat liver parenchymal cells: a biochemical and fine structural study. *J Cell Biol* 43:506-520. doi: 10.1083/jcb.43.3.506
- Brnjic S, Olofsson MH, Havelka AM, Linder S (2010) Chemical biology suggests a role for calcium signaling in mediating sustained JNK activation during apoptosis. *Mol Biosyst* 6:767-774. doi: 10.1039/b920805d
- Byrne AM, Lemasters JJ, Nieminen AL (1999) Contribution of increased mitochondrial free Ca^{2+} to the mitochondrial permeability transition induced by tert-butylhydroperoxide in rat hepatocytes. *Hepatology* 29:1523-1531. doi: 10.1002/hep.510290521
- Chinopoulos C, Dam-Vizi V (2006) Calcium, mitochondria and oxidative stress in neuronal pathology. Novel aspects of an enduring theme. *FEBS J* 273:433-450. doi: 10.1111/j.1742-4658.2005.05103.x

- 1
2
3
4 Cochrane CG (1991) Cellular injury by oxidants. *Am J Med* 91:23S-30S. doi:
5 10.1016/0002-9343(91)90280-B
6
7
8 Colbran RJ (2004) Targeting of calcium/calmodulin-dependent protein kinase II. *Biochem*
9 *J* 378:1-16. doi: 10.1042/BJ20031547
10
11 Davies MJ (1989) Detection of peroxy and alkoxy radicals produced by reaction of
12 hydroperoxides with rat liver microsomal fractions. *Biochem J* 257:603-606. doi:
13 10.1016/0304-4165(88)90063-3
14
15
16 Dimova S, Koleva M, Rangelova D, Stoythchev T (1995) Effect of nifedipine, verapamil,
17 diltiazem and trifluoperazine on acetaminophen toxicity in mice. *Arch Toxicol* 70:112-118.
18 doi: 10.1007/BF02733671
19
20
21 Ding WX, Nam OC (2003) Role of oxidative stress and mitochondrial changes in
22 cyanobacteria-induced apoptosis and hepatotoxicity. *FEMS Microbiol Lett* 220:1-7. doi:
23 10.1016/S0378-1097(03)00100-9
24
25
26 Ding WX, Shen HM, Ong CN (2002) Calpain activation after mitochondrial permeability
27 transition in microcystin-induced cell death in rat hepatocytes. *Biochem Biophys Res*
28 *Commun* 291:321-331. doi: 10.1006/bbrc.2002.6453
29
30
31 Eguchi Y, Shimizu S, Tsujimoto Y (1997) Intracellular ATP levels determine cell death
32 fate by apoptosis or necrosis. *Cancer Res* 57:1835-1840. doi: 10.1001/jama.246.19.2184.
33
34
35 Elrod JW, Molkenin JD (2013) Physiologic functions of cyclophilin D and the
36 mitochondrial permeability transition pore. *Circ J* 77:1111-1122. doi: 10.1253/circj.CJ-13-
37 0321
38
39
40 Erickson JR, Joiner ML, Guan X, Kutschke W, Yang Jet al. (2008) A dynamic pathway for
41 calcium-independent activation of CaMKII by methionine oxidation. *Cell* 133:462-474.
42 10.1016/j.cell.2008.02.048
43
44
45 Fukunaga K, Yoshida M, Nakazono N (1998) A simple, rapid, highly sensitive and
46 reproducible quantification method for plasma malondialdehyde by high-performance
47 liquid chromatography. *Biomed Chromatogr* 12:300-303. doi: 10.1002/(SICI)1099-
48 0801(199809/10)12:5<300::AID-BMC751>3.3.CO;2-R
49
50
51 Griffith OW (1980) Determination of glutathione and glutathione disulfide using
52 glutathione reductase and 2-vinylpyridine. *Anal Biochem* 106:207-212. doi: 10.1016/0003-
53 2697(80)90139-6. doi: 10.1016/0003-2697(80)90139-6
54
55
56 Gryniewicz G, Poenie M, Tsien RY (1985) A new generation of Ca²⁺ indicators with
57 greatly improved fluorescence properties. *J Biol Chem* 260:3440-3450. doi: NOT FOUND
58
59
60 Gschwendt M, Dieterich S, Rennecke J, Kittstein W, Mueller HJ, Johannes FJ (1996)
61 Inhibition of protein kinase C μ by various inhibitors. Differentiation from protein kinase c
62 isoenzymes. *FEBS Lett* 392:77-80. doi: 10.1016/0014-5793(96)00785-5
63
64
65

1
2
3
4 Hajimohammadreza I, Probert AW, Coughenour LL, Borosky SA, Marcoux FW, Boxer
5 PA, Wang KK (1995) A specific inhibitor of calcium/calmodulin-dependent protein kinase-
6 II provides neuroprotection against NMDA- and hypoxia/hypoglycemia-induced cell death.
7 J Neurosci 15:4093-4101. doi: NOT FOUND
8
9

10 Halestrap AP, Doran E, Gillespie JP, O'Toole A (2000) Mitochondria and cell death.
11 Biochem Soc Trans 28:170-177. doi: 10.2174/0929867033457278
12

13 Harper JF, Cheung WY, Wallace RW, Huang HL, Levine SN, Steiner AL (1980)
14 Localization of calmodulin in rat tissues. Proc Natl Acad Sci U S A 77:366-370. doi:
15 10.1073/pnas.77.1.366
16
17

18 Hemenway CS, Heitman J (1999) Calcineurin. Structure, function, and inhibition. Cell
19 Biochem Biophys 30:115-151. doi: 10.1007/BF02737887
20

21 Horbinski C, Chu CT (2005) Kinase signaling cascades in the mitochondrion: a matter of
22 life or death. Free Radic Biol Med 38:2-11. doi: 10.1016/j.freeradbiomed.2004.09.030
23
24

25 Hudmon A, Schulman H (2002) Structure-function of the multifunctional Ca²⁺/calmodulin-
26 dependent protein kinase II. Biochem J 364:593-611. doi: 10.1042/BJ20020228
27
28

29 Imberti R, Nieminen AL, Herman B, Lemasters JJ (1993) Mitochondrial and glycolytic
30 dysfunction in lethal injury to hepatocytes by t-butylhydroperoxide: protection by fructose,
31 cyclosporin A and trifluoperazine. J Pharmacol Exp Ther 265:392-400. doi: NOT FOUND
32

33 Itano T, Matsui H, Doi A, Ohmura Y, Hatase O (1986) Identification of calmodulin-
34 binding proteins in pure mitochondria by photoaffinity labeling. Biochem Int 13:787-792.
35 doi: NOT FOUND
36
37

38 Jeong SY, Seol DW (2008) The role of mitochondria in apoptosis. BMB Rep 41:11-22. doi:
39 10.5483/BMBRep.2008.41.1.011
40

41 Joiner ML, Koval OM, Li J, He BJ, Allamargot Cet al. (2012) CaMKII determines
42 mitochondrial stress responses in heart. Nature 491:269-273. doi: 10.1038/nature11444
43
44

45 Kanno T, Sato EE, Muranaka S, Fujita H, Fujiwara T, Utsumi T, Inoue M, Utsumi K
46 (2004) Oxidative stress underlies the mechanism for Ca²⁺-induced permeability transition
47 of mitochondria. Free Radic Res 38:27-35. doi: 10.1080/10715760310001626266
48
49

50 Kim BJ, Ryu SW, Song BJ (2006) JNK- and p38 kinase-mediated phosphorylation of Bax
51 leads to its activation and mitochondrial translocation and to apoptosis of human hepatoma
52 HepG2 cells. J Biol Chem 281:21256-21265. doi: 10.1074/jbc.M510644200
53
54

55 Korsmeyer SJ, Wei MC, Saito M, Weiler S, Oh KJ, Schlesinger PH (2000) Pro-apoptotic
56 cascade activates BID, which oligomerizes BAK or BAX into pores that result in the
57 release of cytochrome c. Cell Death Differ 7:1166-1173. doi: 10.1038/sj.cdd.4400783
58
59
60
61

1
2
3
4 Kuroda S, Nakai A, Kristian T, Siesjo BK (1997) The calmodulin antagonist trifluoperazine
5 in transient focal brain ischemia in rats. Anti-ischemic effect and therapeutic window.
6 Stroke 28:2539-2544. doi: 10.1161/01.STR.28.12.2539
7

8
9 Lee CS, Park SY, Ko HH, Song JH, Shin YK, Han ES (2005) Inhibition of MPP⁺-induced
10 mitochondrial damage and cell death by trifluoperazine and W-7 in PC12 cells. Neurochem
11 Int 46:169-178. doi: 10.1016/j.neuint.2004.07.007
12

13 Lee KK, Shimoji M, Hossain QS, Sunakawa H, Aniya Y (2008) Novel function of
14 glutathione transferase in rat liver mitochondrial membrane: role for cytochrome c release
15 from mitochondria. Toxicol Appl Pharmacol 232:109-118. doi: 10.1016/j.taap.2008.06.005
16
17

18 Lemasters JJ, Theruvath TP, Zhong Z, Nieminen AL (2009) Mitochondrial calcium and the
19 permeability transition in cell death. Biochim Biophys Acta 1787:1395-1401. doi:
20 10.1016/j.bbabi.2009.06.009
21

22
23 Li J, Wang P, Yu S, Zheng Z, Xu X (2012) Calcium entry mediates hyperglycemia-induced
24 apoptosis through Ca²⁺/calmodulin-dependent kinase II in retinal capillary endothelial cells.
25 Mol Vis 18:2371-2379. doi: NOT FOUND
26

27 Liu G, Zhao J, Chang Z, Guo G (2013) CaMKII activates ASK1 to induce apoptosis of
28 spinal astrocytes under oxygen-glucose deprivation. Cell Mol Neurobiol 33:543-549. doi:
29 10.1007/s10571-013-9920-0
30
31

32 Liu Y, Templeton DM (2007) Cadmium activates CaMK-II and initiates CaMK-II-
33 dependent apoptosis in mesangial cells. FEBS Lett 581:1481-1486. doi:
34 0.1016/j.febslet.2007.03.003
35
36

37 Lowry OH, Rosebrough NJ, Farr AL, Randall RJ (1951) Protein measurement with the
38 Folin phenol reagent. J Biol Chem 193:265-275. doi: NOT FOUND
39

40 Lyman GE, DeVincenzo JP (1967) Determination of picogram amounts of ATP using the
41 luciferin-luciferase enzyme system. Anal Biochem 21:435-443. doi: 10.1016/0003-
42 2697(67)90318-1
43
44

45 Majumder PK, Mishra NC, Sun X, Bharti A, Kharbanda S, Saxena S, Kufe D (2001)
46 Targeting of protein kinase C delta to mitochondria in the oxidative stress response. Cell
47 Growth Differ 12:465-470. doi: NOT FOUND
48
49

50 McClelland P, Adam LP, Hathaway DR (1994) Identification of a latent Ca²⁺/calmodulin
51 dependent protein kinase II phosphorylation site in vascular calpain II. J Biochem 115:41-
52 46. doi: NOT FOUND
53
54

55 Molkenin JD (2001) Calcineurin, mitochondrial membrane potential, and cardiomyocyte
56 apoptosis. Circ Res 88:1220-1222. doi: NOT FOUND
57

58 Muriel P (2009) Role of free radicals in liver diseases. Hepatol Int 3:526-536. doi:
59 10.1007/s12072-009-9158-6
60
61

1
2
3
4 Nguyen A, Chen P, Cai H (2004) Role of CaMKII in hydrogen peroxide activation of
5 ERK1/2, p38 MAPK, HSP27 and actin reorganization in endothelial cells. FEBS Lett
6 572:307-313. doi: 10.1016/j.febslet.2004.06.061
7

8
9 Nieminen AL, Byrne AM, Herman B, Lemasters JJ (1997) Mitochondrial permeability
10 transition in hepatocytes induced by t-BuOOH: NAD(P)H and reactive oxygen species. Am
11 J Physiol 272:C1286-C1294. doi: NOT FOUND
12

13
14 Nieminen AL, Saylor AK, Tesfai SA, Herman B, Lemasters JJ (1995) Contribution of the
15 mitochondrial permeability transition to lethal injury after exposure of hepatocytes to t-
16 butylhydroperoxide. Biochem J 307 (Pt 1):99-106. doi: 10.1016/0270-9139(93)92139-Q
17

18
19 Odagiri K, Katoh H, Kawashima H, Tanaka T, Ohtani H, Saotome M, Urushida T, Satoh H,
20 Hayashi H (2009) Local control of mitochondrial membrane potential, permeability
21 transition pore and reactive oxygen species by calcium and calmodulin in rat ventricular
22 myocytes. J Mol Cell Cardiol 46:989-997. doi: 10.1016/j.yjmcc.2008.12.022
23

24
25 Orrenius S, Burkitt MJ, Kass GE, Dypbukt JM, Nicotera P (1992) Calcium ions and
26 oxidative cell injury. Ann Neurol 32 Suppl:S33-S42. doi: 10.1002/ana.410320708
27

28
29 Orrenius S, Gogvadze V, Zhivotovsky B (2007) Mitochondrial oxidative stress:
30 implications for cell death. Annu Rev Pharmacol Toxicol 47:143-183. doi:
31 10.1146/annurev.pharmtox.47.120505.105122
32

33
34 Perez LM, Milkiewicz P, Ahmed-Choudhury J, Elias E, Ochoa JE, Sanchez Pozzi EJ,
35 Coleman R, Roma MG (2006) Oxidative stress induces actin-cytoskeletal and tight-
36 junctional alterations in hepatocytes by a Ca²⁺-dependent, PKC-mediated mechanism:
37 protective effect of PKA. Free Radic Biol Med 40:2005-2017. doi:
38 10.1016/j.freeradbiomed.2006.01.034
39

40
41 Rich DP, Schworer CM, Colbran RJ, Soderling TR (1990) Proteolytic activation of
42 calcium/calmodulin-dependent protein kinase II: Putative function in synaptic plasticity.
43 Mol Cell Neurosci 1:107-116. doi: NOT FOUND
44

45
46 Ronco MT, Alvarez ML, Monti JA, Carrillo MC, Pisani GB, Lugano MC, Carnovale CE
47 (2004) Role of nitric oxide increase on induced programmed cell death during early stages
48 of rat liver regeneration. Biochim Biophys Acta 1690:70-76. doi:
49 10.1016/j.bbadis.2004.05.004
50

51
52 Roy DN, Mandal S, Sen G, Biswas T (2009) Superoxide anion mediated mitochondrial
53 dysfunction leads to hepatocyte apoptosis preferentially in the periportal region during
54 copper toxicity in rats. Chem Biol Interact 182:136-147. doi: 10.1016/j.cbi.2009.08.014
55

56
57 Ruvolo PP, Deng X, Carr BK, May WS (1998) A functional role for mitochondrial protein
58 kinase C α in Bcl2 phosphorylation and suppression of apoptosis. J Biol Chem 273:25436-
59 25442. doi: 10.1074/jbc.273.39.25436
60
61
62
63
64
65

1
2
3
4 Scaduto RC, Jr., Grotyohann LW (1999) Measurement of mitochondrial membrane
5 potential using fluorescent rhodamine derivatives. *Biophys J* 76:469-477. doi:
6 10.1016/S0006-3495(99)77214-0
7

8
9 Schwertz H, Carter JM, Abdudurehman M, Russ M, Buerke U et al. (2007) Myocardial
10 ischemia/reperfusion causes VDAC phosphorylation which is reduced by cardioprotection
11 with a p38 MAP kinase inhibitor. *Proteomics* 7:4579-4588. doi: 10.1002/pmic.200700734
12

13 Takano H, Fukushi H, Morishima Y, Shirasaki Y (2003) Calmodulin and calmodulin-
14 dependent kinase II mediate neuronal cell death induced by depolarization. *Brain Res*
15 962:41-47. doi: 10.1016/S0006-8993(02)03932-X
16

17
18 Takeyama N, Matsuo N, Tanaka T (1993) Oxidative damage to mitochondria is mediated
19 by the Ca²⁺-dependent inner-membrane permeability transition. *Biochem J* 294 (Pt 3):719-
20 725. doi: NOT FOUND
21

22
23 Thor H, Hartzell P, Orrenius S (1984) Potentiation of oxidative cell injury in hepatocytes
24 which have accumulated Ca²⁺. *J Biol Chem* 259:6612-6615. doi: NOT FOUND
25

26
27 Tietze F (1969) Enzymic method for quantitative determination of nanogram amounts of
28 total and oxidized glutathione: applications to mammalian blood and other tissues. *Anal*
29 *Biochem* 27:502-522. doi: 10.1016/0003-2697(69)90064-5
30

31 Timmins JM, Ozcan L, Seimon TA, Li G, Malagelada C et al. (2009) Calcium/calmodulin-
32 dependent protein kinase II links ER stress with Fas and mitochondrial apoptosis pathways.
33 *J Clin Invest* 119:2925-2941. doi: 10.1172/JCI38857
34

35
36 Tsuruta F, Sunayama J, Mori Y, Hattori S, Shimizu S, Tsujimoto Y, Yoshioka K,
37 Masuyama N, Gotoh Y (2004) JNK promotes Bax translocation to mitochondria through
38 phosphorylation of 14-3-3 proteins. *EMBO J* 23:1889-1899. doi:
39 10.1038/sj.emboj.7600194
40

41
42 Tzung SP, Fausto N, Hockenbery DM (1997) Expression of Bcl-2 family during liver
43 regeneration and identification of Bcl-x as a delayed early response gene. *Am J Pathol*
44 150:1985-1995. doi: NOT FOUND
45

46
47 Vercesi AE, Kowaltowski AJ, Oliveira HC, Castilho RF (2006) Mitochondrial Ca²⁺
48 transport, permeability transition and oxidative stress in cell death: implications in
49 cardiotoxicity, neurodegeneration and dyslipidemias. *Front Biosci* 11:2554-2564. doi:
50 10.2741/1990
51

52
53 Vermes I, Haanen C, Steffens-Nakken H, Reutelingsperger C (1995) A novel assay for
54 apoptosis. Flow cytometric detection of phosphatidylserine expression on early apoptotic
55 cells using fluorescein labelled Annexin V. *J Immunol Methods* 184:39-51. doi:
56 10.1016/0022-1759(95)00072-I
57

1
2
3
4 Villarruel MC, Fernandez G, de Ferreyra EC, de Fenos OM, Castro JA (1990) Modulation
5 of the course of CCl₄-induced liver injury by the anti-calmodulin drug thioridazine. Toxicol
6 Lett 51:13-21. doi: NOT FOUND
7

8
9 Wang HG, Pathan N, Ethell IM, Krajewski S, Yamaguchi Yet al. (1999) Ca²⁺-induced
10 apoptosis through calcineurin dephosphorylation of BAD. Science 284:339-343. doi:
11 10.1126/science.284.5412.339
12

13
14 Yaglom JA, Ekhterae D, Gabai VL, Sherman MY (2003) Regulation of necrosis of H9c2
15 myogenic cells upon transient energy deprivation. Rapid deenergization of mitochondria
16 precedes necrosis and is controlled by reactive oxygen species, stress kinase JNK, HSP72
17 and ARC. J Biol Chem 278:50483-50496. doi: 10.1074/jbc.M306903200
18

19
20 Yuen EY, Liu W, Yan Z (2007) The phosphorylation state of GluR1 subunits determines
21 the susceptibility of AMPA receptors to calpain cleavage. J Biol Chem 282:16434-16440.
22 doi: 10.1074/jbc.M701283200
23
24
25
26
27
28
29
30
31
32
33
34
35
36
37
38
39
40
41
42
43
44
45
46
47
48
49
50
51
52
53
54
55
56
57
58
59
60
61
62
63
64
65

1
2
3
4
5
6 **Table-1**

7
8 *Effect of tBOOH on cellular integrity, redox status and Ca²⁺ levels*

9
10
11

	DMSO ^a	tBOOH ^b
Cellular viability (% of total cells)	96 ± 3	62 ± 3*
LDH release (% of total cell content)	32 ± 2	42 ± 3*
ATP cellular content (µmol/10 ⁶ cells)	48 ± 6	43 ± 3
MDA cellular content /nmol/mg prot.)	1.3 ± 0,2	8,0 ± 0,3*
Total glutathione (mg/mg of protein)	27 ± 2	17 ± 1*
GSSG-to-total glutathione ratio (%)	3,1 ± 0,1	4,1 ± 0,2*
Cytosolic free Ca ²⁺ (nM)	119 ± 11	3029 ± 474*

12
13
14
15
16
17
18
19
20
21
22
23
24
25
26
27
28
29
30
31
32
33
34

35 Cells were pretreated for 15 min either with tBOOH (500 µM) or DMSO (controls).

36
37 *Note:* LDH, lactate dehydrogenase; ATP, adenosine triphosphate; MDA,
38 malondialdehyde; GSSG, oxidized glutathione.

39
40 * p < 0.05 vs. DMSO, for n = 4-10.
41
42
43
44
45
46
47
48
49
50
51
52
53
54
55
56
57
58
59
60
61
62
63
64
65

FIGURE LEGENDS

Figure 1. *Involvement of Ca^{2+} and signalling molecules acting downstream of Ca^{2+} in *tBOOH*-induced mitochondrial permeability transition (MPT), and the subsequent malondialdehyde (MDA) formation. (A) Effect of the intracellular Ca^{2+} chelator BAPTA/AM (50 μ M), the antagonists of CaM trifluoperazine (TFP, 10 μ M) and W7 (100 μ M; with or without 5 μ M cyclosporin A-CsA), the calcineurin inhibitor FK-506 (1 μ M), or the CaMKII inhibitor KN-62 (10 μ M) on *tBOOH* (500 μ M, 15 min)-induced MPT, as assessed by measuring mitochondrial membrane depolarization as a surrogate marker, using tetra-methyl-rhodamine methyl ester as a fluorescent probe. Mitochondrial membrane depolarization was expressed as the percentage of the change in mitochondrial depolarization, in a scale ranging from a basal, non-depolarized condition (control value) to the maximal depolarized condition, obtained by adding the respiratory chain uncoupling compound, carbonyl cyanide *m*-chloro-phenylhydrazone (10 μ M). The dotted line represents the mean value of the change in mitochondrial $\Delta\psi$ induced by *tBOOH* in hepatocytes pretreated with the MPTP blocker CsA ($54 \pm 3\%$); the differences of the values of the different experimental groups with this reference value reflects MPT-dependent changes in mitochondrial $\Delta\psi$. (B) Effect of these pre-treatments on *tBOOH*-induced LPO, as evaluated by measuring MDA formation. The dotted line represents the mean value of the MDA content in CsA-pretreated hepatocytes exposed to *tBOOH* ($54 \pm 3\%$); the differences of the values of the different experimental groups with this reference value reflects MPT-dependent MDA formation.*

Note that BAPTA, the CaM antagonists and the CaMKII inhibitor prevented partially both MPTP and MDA formation to the same extent as the MPT blocker CsA did, suggesting that

1
2
3
4 MPTP formation and the subsequent LPO are facilitated by Ca^{+2} elevations, and this
5
6 phenomena are modulated by CaM via CaMKII activation. Contrarily, the calcineurin
7
8 inhibitor FK-506 was without effect, suggesting that calcineurin play no role in *t*BOOH
9
10 effects.
11
12

13
14 Values are mean \pm SE, for 4-10 independent experiments. ^aSignificantly different from
15
16 control ($p < 0.05$); ^bsignificantly different from *t*BOOH-treated cells ($p < 0.05$).
17
18
19
20
21

22
23 **Figure 2.** *Activation by phosphorylation of CaMKII by tBOOH, and its prevention by CaM*
24
25 *and CaMKII inhibition. Upper panel:* Representative Western blottings of phospho (p)-
26
27 CaMKII and total CaMKII content in whole cellular lysates of cultured rat hepatocytes,
28
29 exposed to *t*BOOH (500 μM , 15 min), with or without a 15-min pre-treatment with the
30
31 CaM antagonists trifluorperazine (TFP, 10 μM) and W7 (100 μM), or with the CaMKII
32
33 inhibitor KN-62 (10 μM). *Lower panel:* CaMKII phosphorylation status for each
34
35 experimental condition, expressed as the phosphorylated-to-total CaMKII ratio, and
36
37 referred to control values. Results are mean \pm SE, for 5 independent experiments.
38
39
40
41
42 ^aSignificantly different from control ($p < 0.05$); ^bsignificantly different from *t*BOOH-treated
43
44 cells ($p < 0.05$).
45
46
47
48
49

50
51 **Figure 3.** *Activation by phosphorylation of JNK1/2 and p38^{MAPK} by tBOOH, and its*
52
53 *prevention by intracellular Ca²⁺ chelation and CaM/CaMKII inhibition. Upper panels:*
54
55 Representative Western blottings of (A) phospho (p)-JNK1/2 and (B) p-p38 MAPK, and of
56
57 the total content of these MAPK in whole lysates of cultured rat hepatocytes, exposed to
58
59 *t*BOOH (500 μM , 15 min), with or without a 15-min pre-treatment with the Ca^{2+} chelating
60
61
62
63
64
65

1
2
3
4 agent BAPTA/AM (50 μ M), the CaM antagonists trifluorperazine (TFP, 10 μ M) and W7
5
6 (100 μ M), or the CaMKII inhibitor KN-62 (10 μ M). *Lower panels:* JNK1/2 and p38^{MAPK}
7
8 phosphorylation status for each experimental condition, expressed as the phosphorylated-
9
10 to-total ratio, and referred to control values. Results are mean \pm SE, for 4 independent
11
12 experiments. ^aSignificantly different from control ($p < 0.05$); ^bsignificantly different from
13
14 *t*BOOH-treated cells ($p < 0.05$).
15
16
17
18
19
20
21

22 **Figure 4.** *Involvement of the Ca²⁺/CaM/CaMKII signaling pathway in tBOOH-induced*
23
24 *apoptosis.* Apoptosis was assessed with annexin V-FITC and propidium iodide (PI)
25
26 staining, by using flow cytometry analysis. Cells in culture were incubated with *t*BOOH
27
28 (500 μ M, 15 min), with or without a 15-min pre-treatment with the mitochondrial
29
30 permeability transition blocker cyclosporin A (CsA, 5 μ M), the intracellular Ca²⁺ chelator
31
32 BAPTA/AM (50 μ M), the CaM antagonists trifluorperazine (TFP, 10 μ M) and W7 (100
33
34 μ M), or the CaMKII inhibitor KN-62 (10 μ M). The percentages of cells (referred to control
35
36 values) with early apoptosis [annexin V (+)/PI (-)], with late apoptosis [annexin V (+)/PI
37
38 (+)], or with any stage of apoptosis [annexin V (+)], are depicted in the panels A, B, and C,
39
40 respectively. Results represent mean \pm SEM of 3 experiments. ^aSignificantly different from
41
42 control ($p < 0.05$); ^bsignificantly different from *t*BOOH-treated cells ($p < 0.05$).
43
44
45
46
47
48
49
50
51
52

53 **Figure 5.** *Involvement of the Ca²⁺/CaM/CaMKII signaling pathway in tBOOH-induced*
54
55 *mitochondrial release of cytochrome c.* *Upper panel:* Representative Western blottings of
56
57 cytochrome *c* content in the cytosolic fraction of cultured rat hepatocytes exposed to
58
59 *t*BOOH (500 μ M, 15 min), with or without a 15-min pre-treatment with the CaM antagonist
60
61
62
63
64
65

1
2
3
4 W7 (100 μM), or with the CaMKII inhibitor KN-62 (10 μM); β -actin was used as loading
5 control. *Lower panel:* Densitometric analysis of cytochrome *c* electrophoretic bands for
6 each experimental condition, referred to the respective signal intensity of β -actin, and
7 expressed as percentage of control values. Data are mean \pm SE for 5 separate experiments.
8
9
10
11
12
13
14 ^aSignificantly different from control ($p < 0.05$); ^bsignificantly different from *t*BOOH-
15 treated cells ($p < 0.05$).
16
17
18
19
20
21

22 **Figure 6.** *Involvement of the Ca²⁺/CaM/CaMKII signaling pathway in tBOOH-induced*
23 *activation of caspase-3.* Activity of caspase-3 in cultured cells exposed to *t*BOOH (500
24 μM , 15 min), with or without a 15-min pre-treatment with the mitochondrial permeability
25 transtion blocker cyclosporin A (CsA, 5 μM), the intracellular Ca²⁺ chelator BAPTA/AM
26 (50 μM), the CaM antagonists trifluorperazine (TFP, 10 μM) and W7 (100 μM), or the
27 CaMKII inhibitor KN-62 (10 μM). Caspase-3 activity was determined by using a
28 fluorometric assay, as described in *Material and Methods* Section. Bars represent activity
29 expressed as percentage of control values. Data are mean \pm SE for 4 independent
30 experiments. ^aSignificantly different from control group ($p < 0.05$); ^bsignificantly different
31 from *t*BOOH-treated cells ($p < 0.05$).
32
33
34
35
36
37
38
39
40
41
42
43
44
45
46
47
48
49

50 **Figure 7.** *Involvement of the Ca²⁺/CaM/CaMKII signaling pathway in tBOOH-induced*
51 *increase in the Bax-to-Bcl-xL ratio.* *Upper panel:* Representative Western blottings of Bax
52 and Bcl-xL illustrating their protein expressions in the mitochondrial fraction of cultured rat
53 hepatocytes exposed to *t*BOOH (500 μM , 15 min), with or without a 15-min pre-treatment
54 with the CaM antagonist W7 (100 μM), or the CaMKII inhibitor KN-62 (10 μM);
55
56
57
58
59
60
61
62
63
64
65

1
2
3
4 prohibitin was used as a mitochondrial protein loading control. *Lower panel:* Bax-to-Bcl-
5
6 xL ratio for each experimental condition, calculated from the densitometric analysis of the
7
8 electrophoretic bands of these proteins normalized to the respective signal intensity of
9
10 prohibitin, and expressed as percentage of controls. Data are mean \pm SE for 3 independent
11
12 experiments. ^aSignificantly different from control group ($p < 0.05$); ^bsignificantly different
13
14 from *t*BOOH-treated cells ($p < 0.05$).
15
16
17
18
19
20
21

22 **Figure 8.** *Effect of CaM and CaMKII antagonists on tBOOH-induced swelling of isolated*
23
24 *rat liver mitochondria.* Mitochondria were suspended at a concentration of 0.5 mg of
25
26 protein/ml, and a 2-min baseline of light scattering at 540 nm was obtained. Then, *t*BOOH
27
28 (500 μ M final concentration) was added to the swelling buffer, together (or not) with the
29
30 mitochondrial permeability transition blocker cyclosporin A (CsA, 5 μ M), the CaM
31
32 antagonist W7 (100 μ M), or the CaMKII inhibitor KN-62 (10 μ M). Changes in light
33
34 scattering at 540 nm were then recorded at 30-s intervals for 15 min. Data are mean \pm SE
35
36 for 8-16 independent experiments. * $p < 0.005$; # $p < 0.001$.
37
38
39
40
41
42
43
44

45 **Figure 9.** *Schematic representation of the main conclusions drawn from this study.* The
46
47 Ca^{2+} -calmodulin (CaM)-dependent protein kinase type II (CaMKII) signaling pathway
48
49 mediates the facilitating role of oxidative-stress-induced Ca^{2+} mitochondrial permeability
50
51 transition via both the onset of the mitochondrial permeability transition pore (MPTP),
52
53 probably via p38^{MAPK} (p38) activation, and Bax translocation to mitochondria, probably via
54
55 JNK activation. Disruption of the mitochondrial permeability barrier leads to: a)
56
57
58
59
60
61
62
63
64
65 impairment of the mitochondrial electron transport chain with leakage of electrons and

1
2
3
4
5
6
7
8
9
10
11
12
13
14
15
16
17
18
19
20
21
22
23
24
25
26
27
28
29
30
31
32
33
34
35
36
37
38
39
40
41
42
43
44
45
46
47
48
49
50
51
52
53
54
55
56
57
58
59
60
61
62
63
64
65

subsequent ROS generation from mitochondrial origin, which contributes to the amplification/perpetuation of the oxidative damage, and *b*) hepatocellular death by apoptosis via the mitochondrial pathway, due to the mitochondrial pore-mediated release of cytochrome *c* (Cyt *c*), followed by apoptosome formation and activation of caspase-3 (Casp-3).

Figure 1
[Click here to download high resolution image](#)

Figure 1

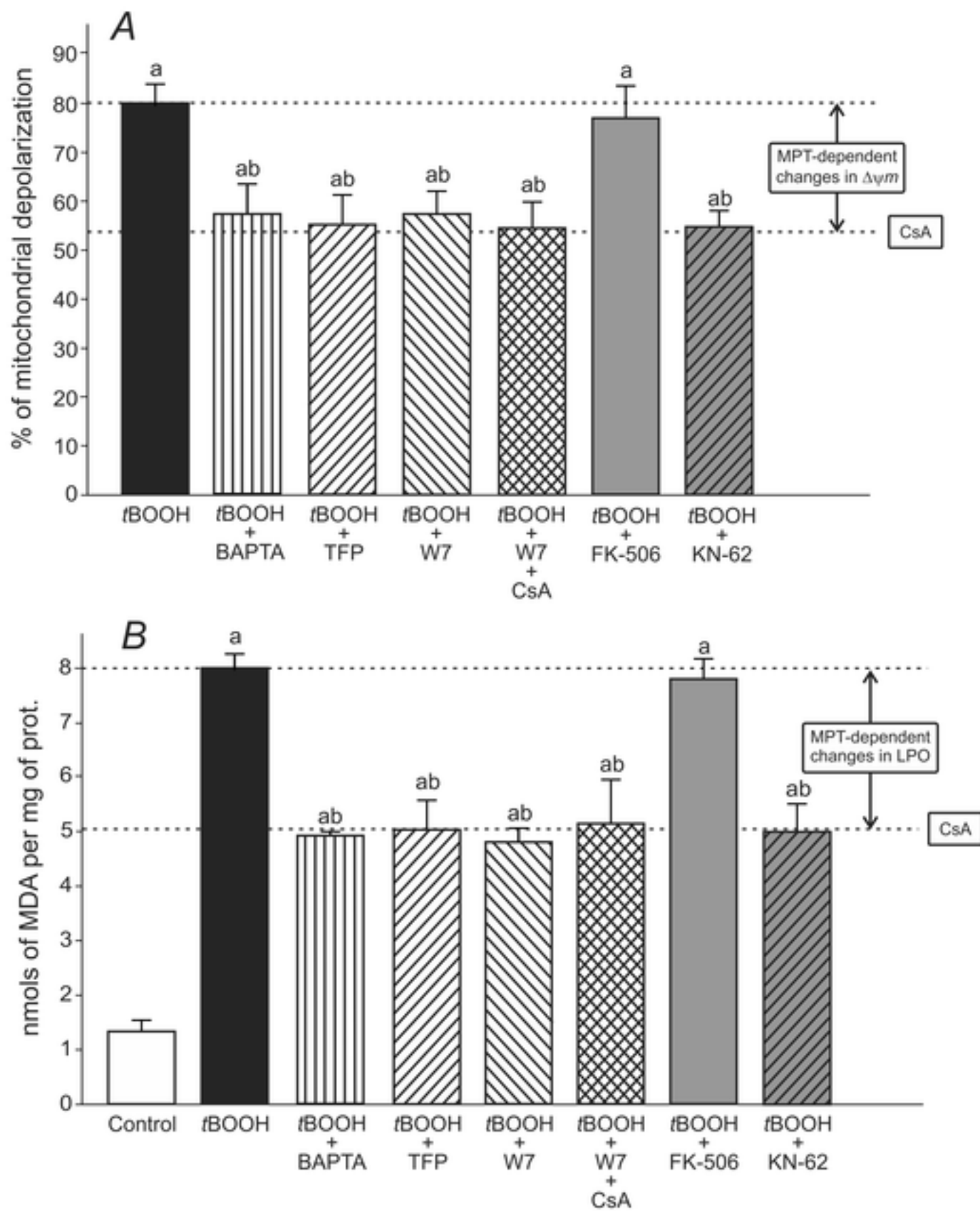


Figure 2

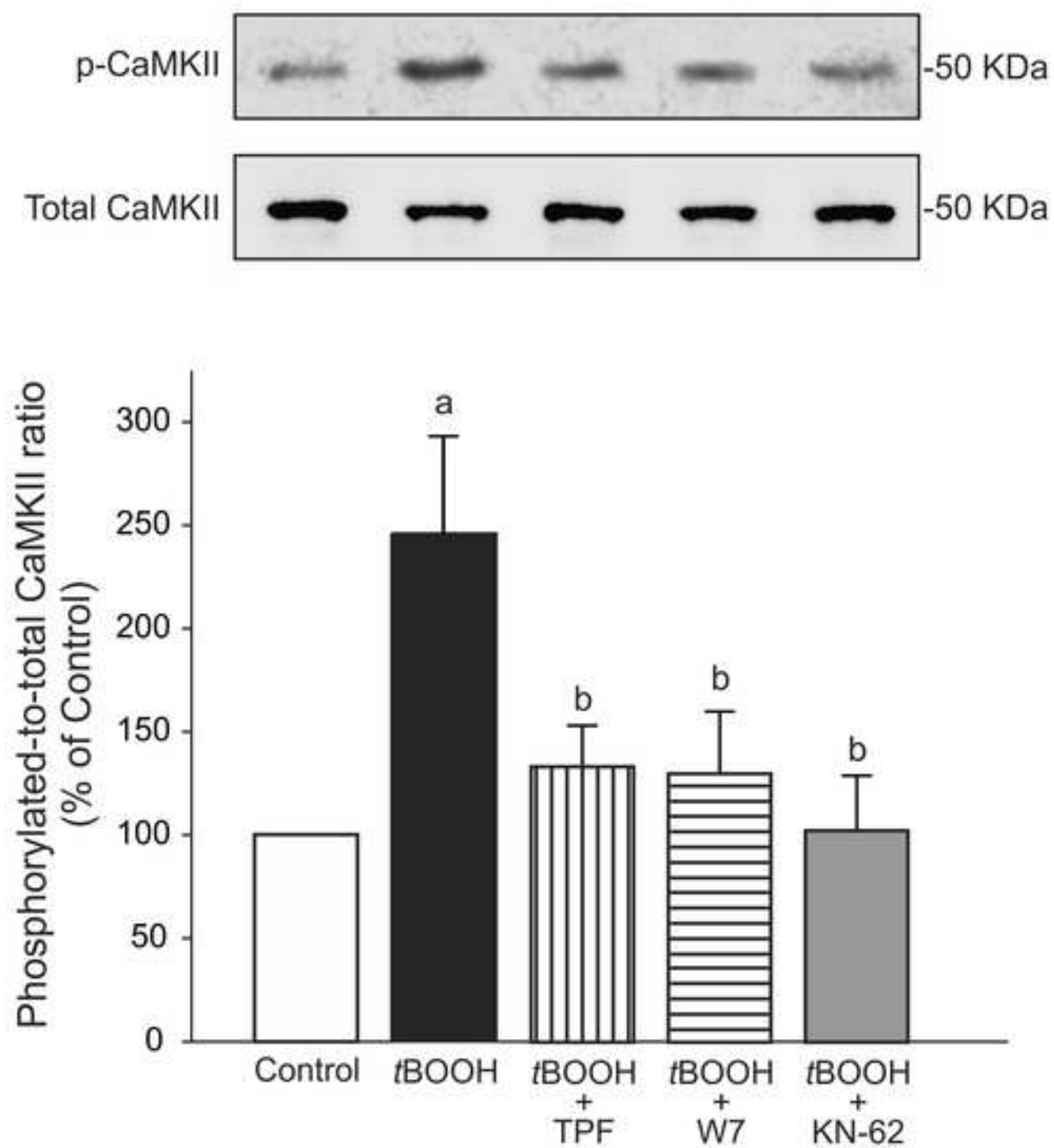
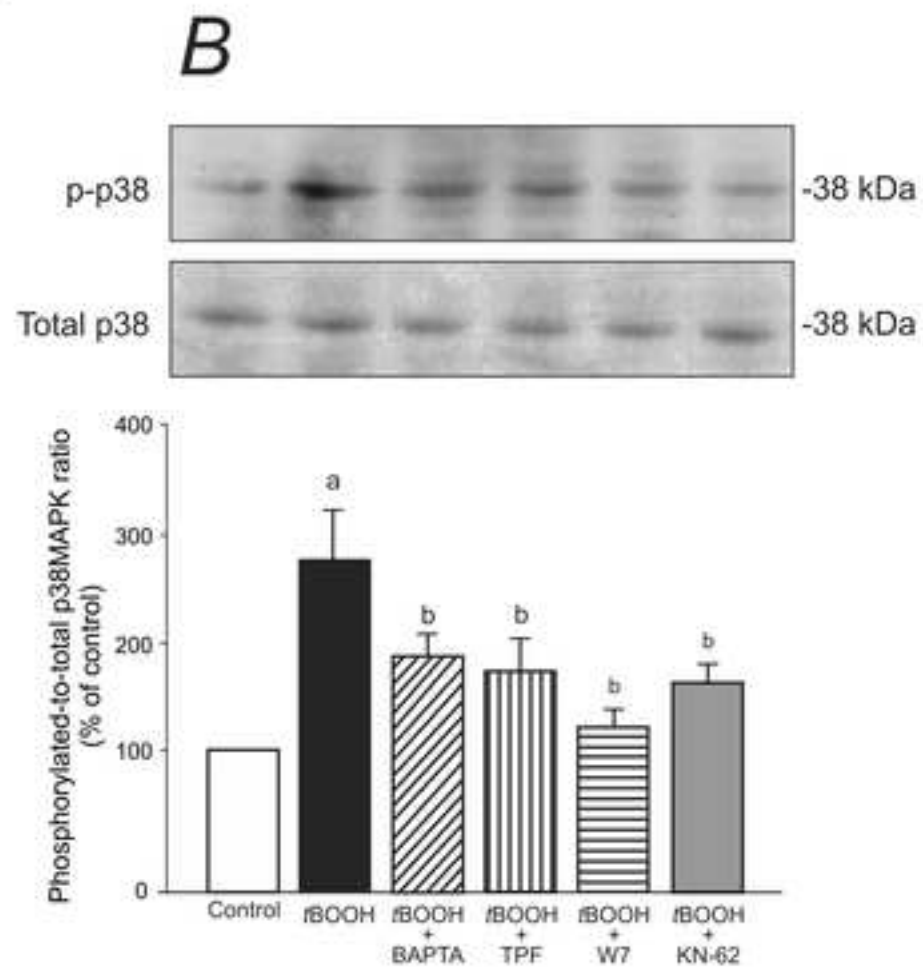
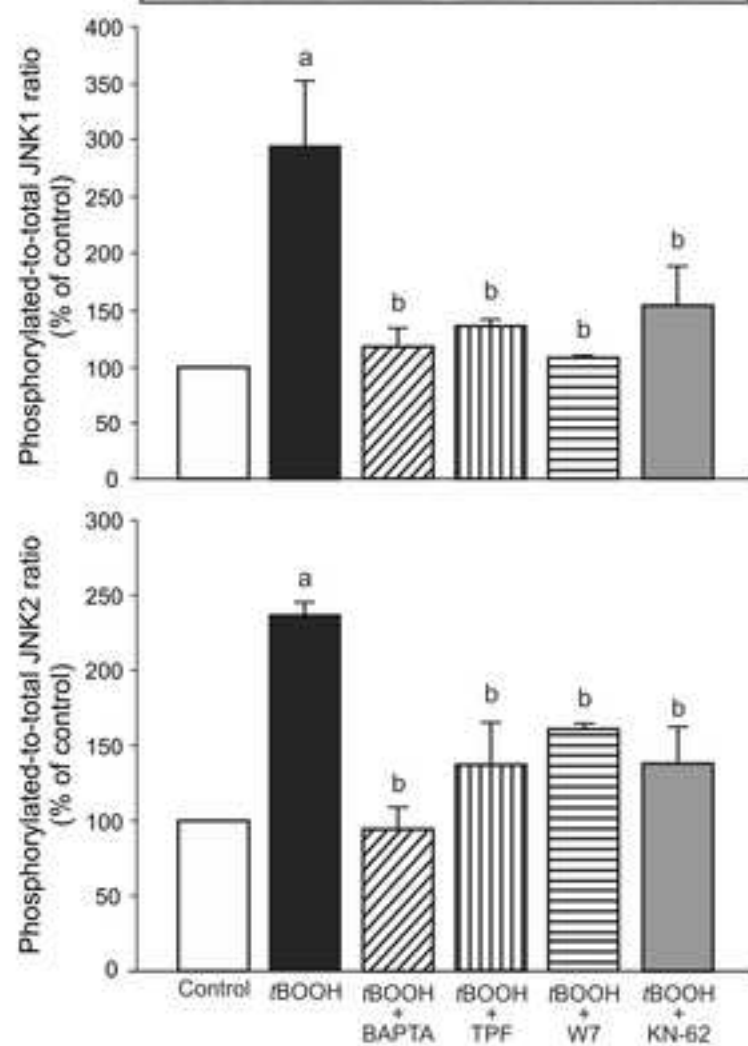


Figure 3
[Click here to download high resolution image](#)



Figure 3



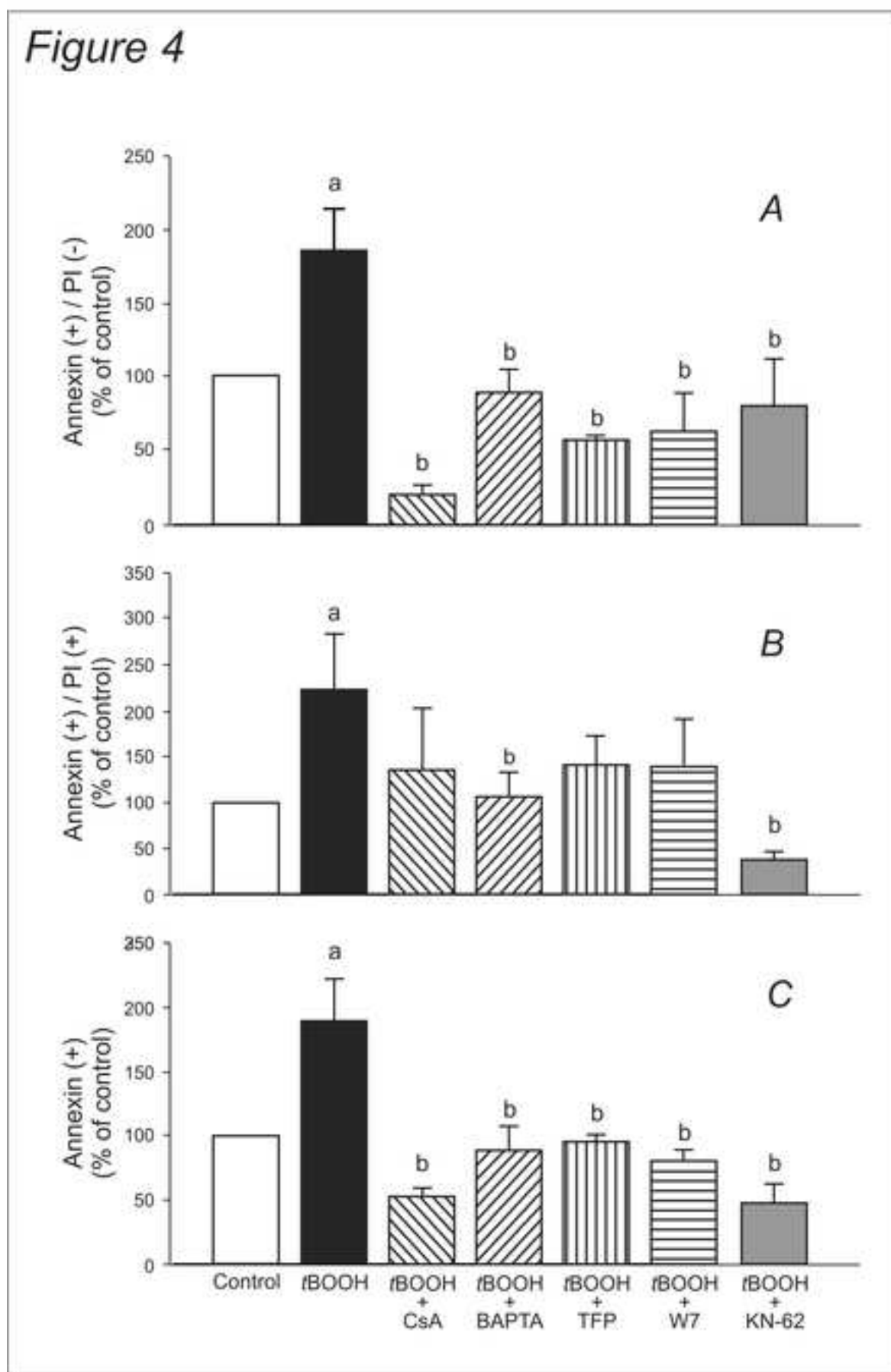


Figure 5

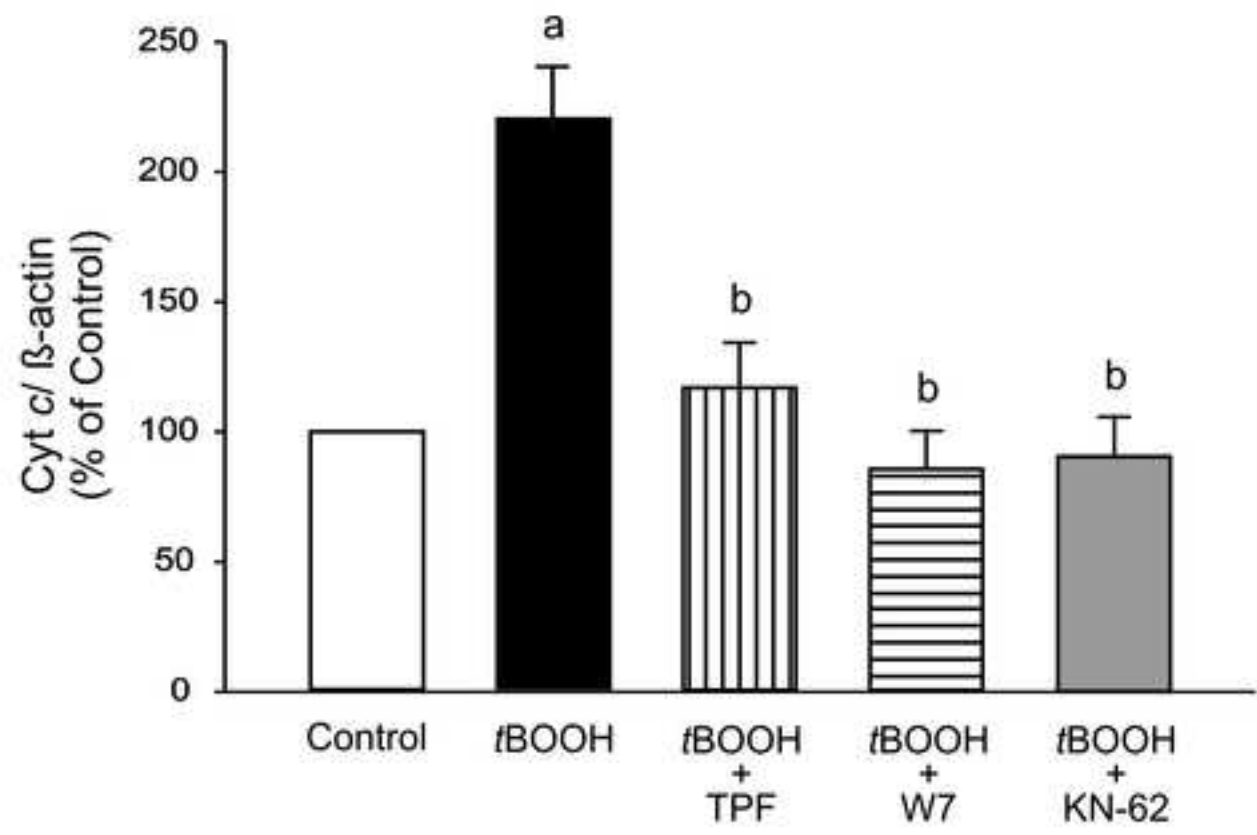
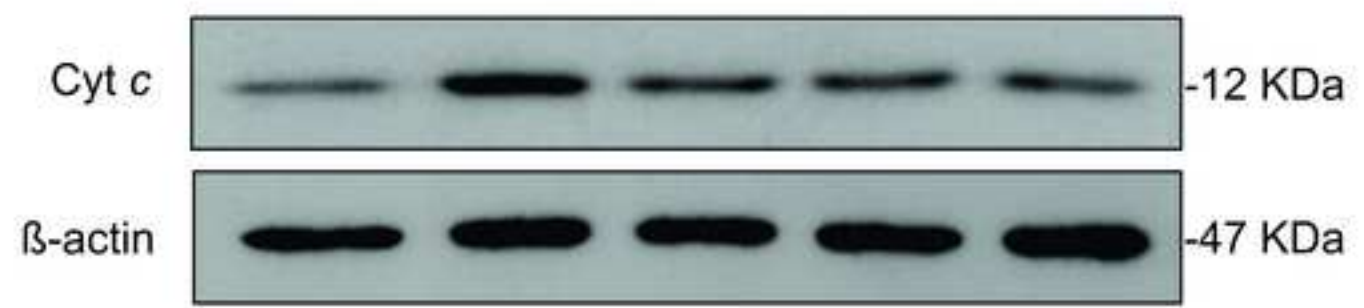


Figure 6

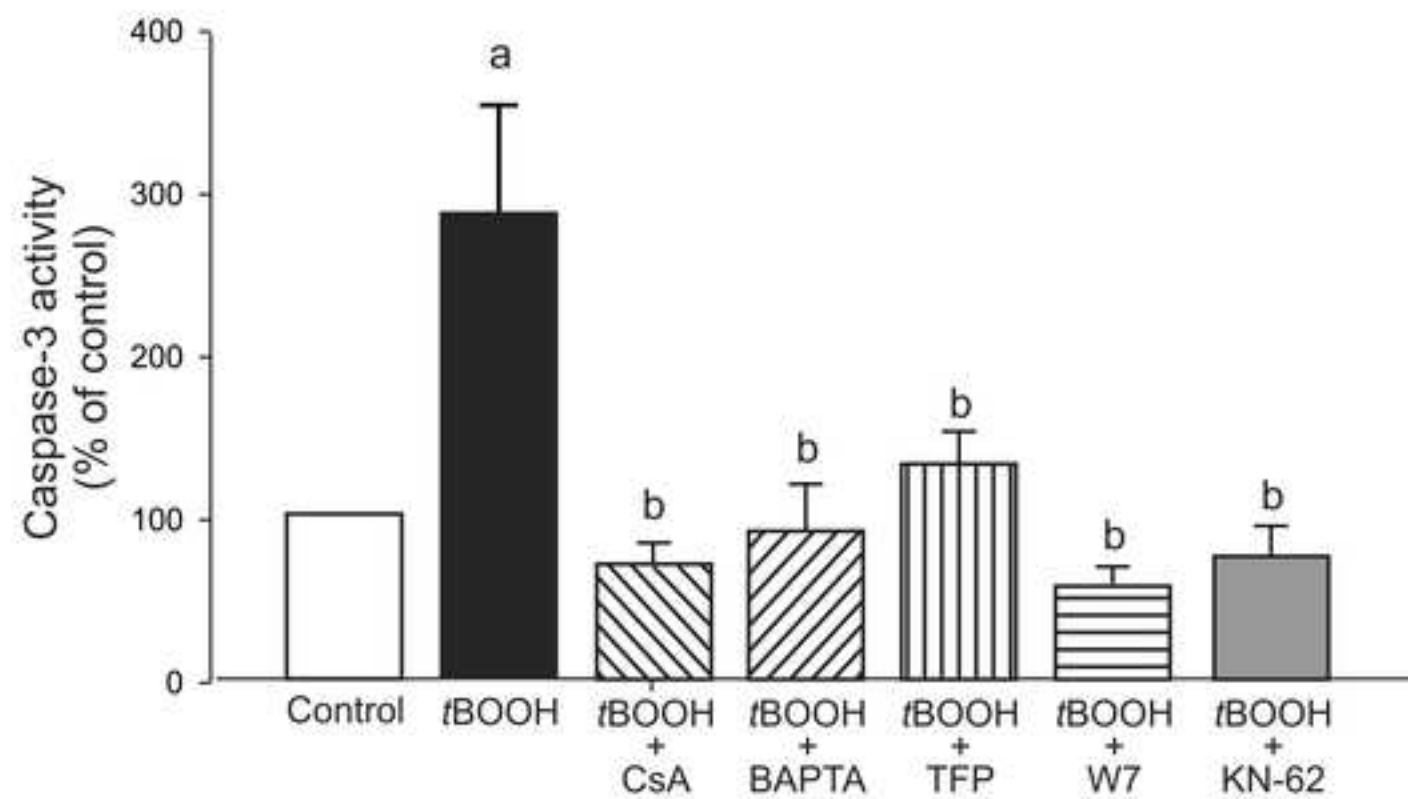


Figure 7

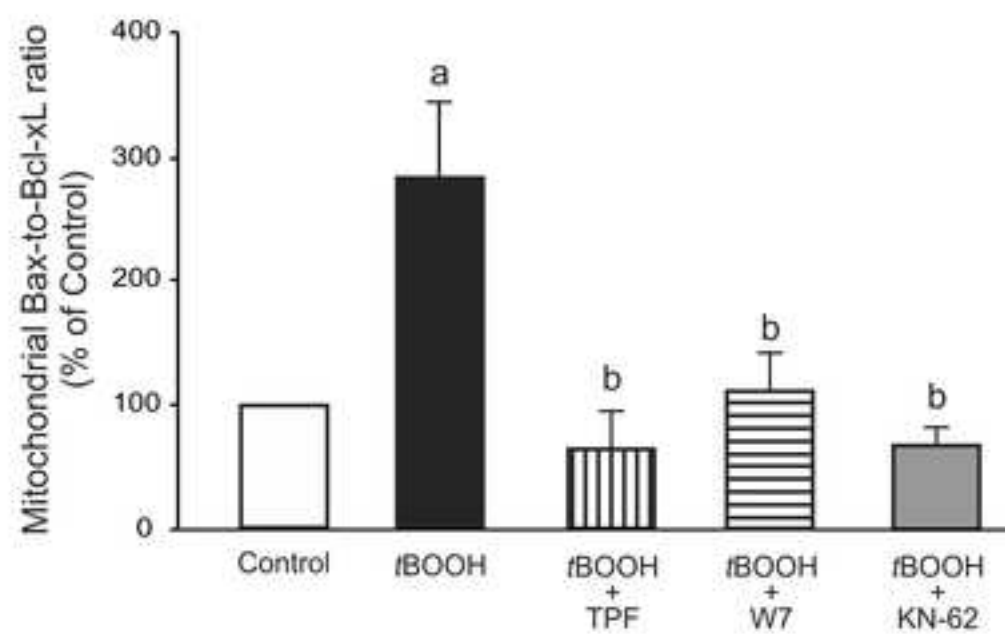
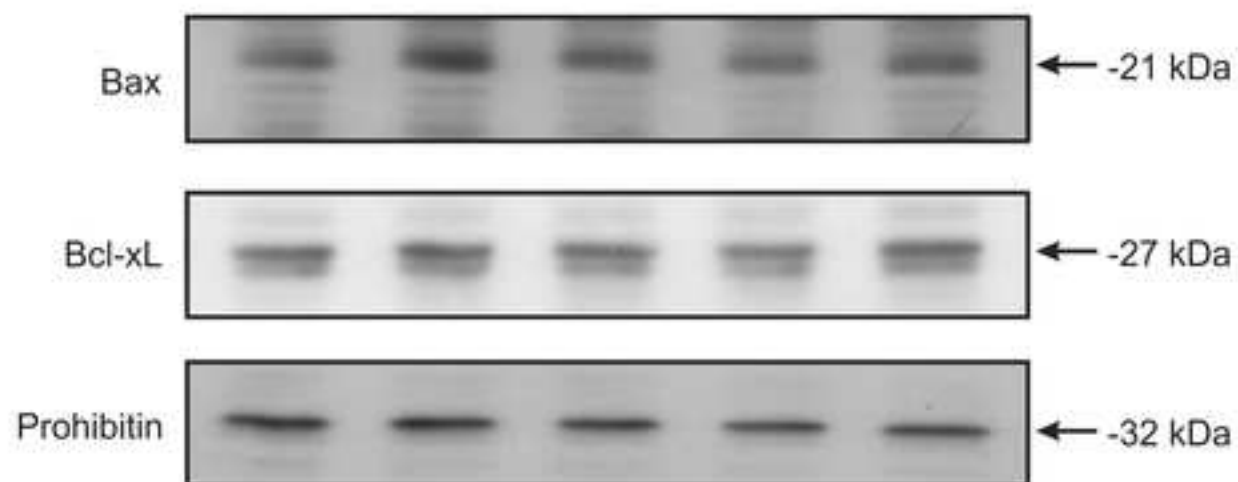


Figure 8
[Click here to download high resolution image](#)

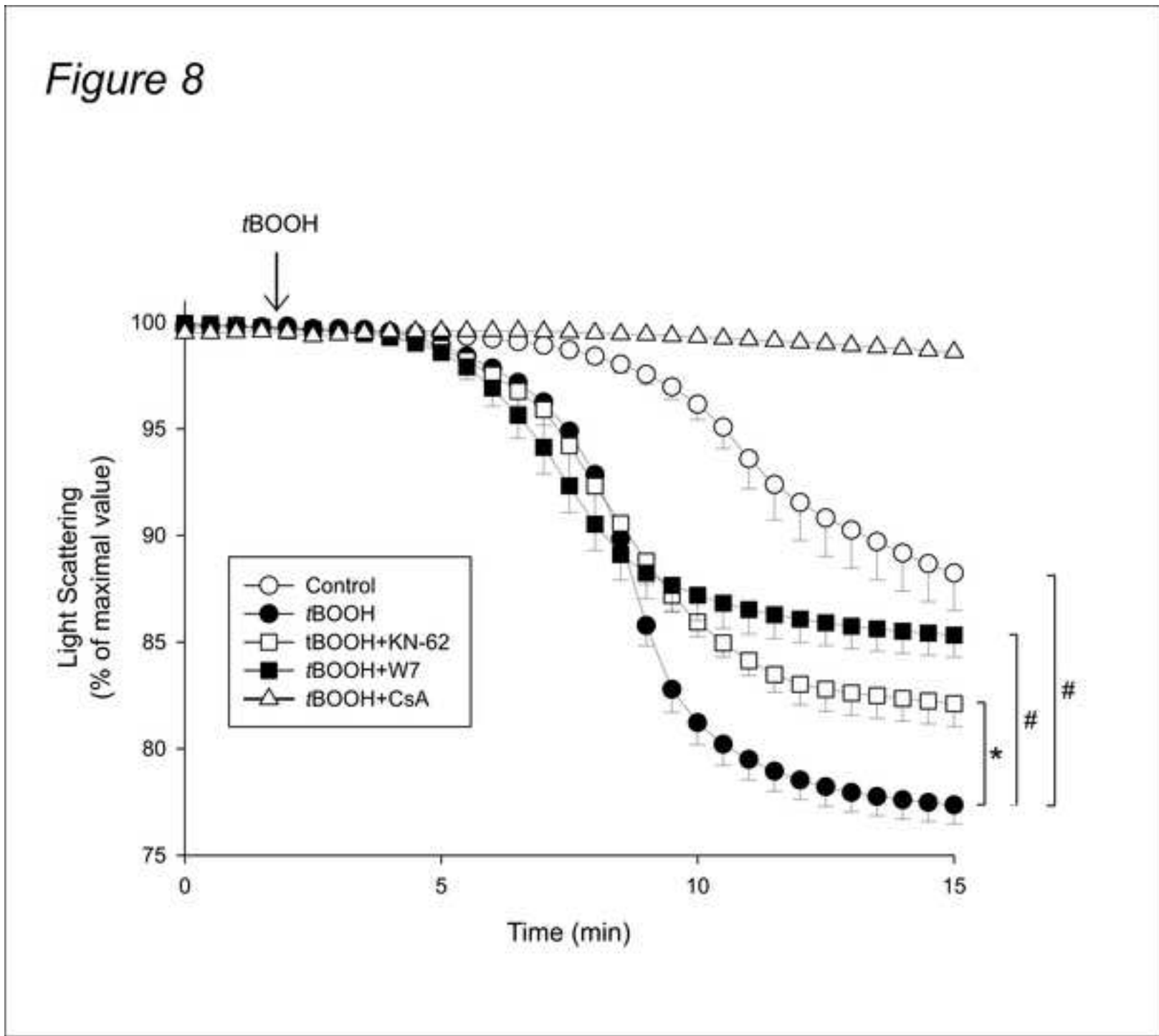


Figure 9
[Click here to download high resolution image](#)

Figure 9

